



# Mapping the world's inland surface waters: an update to the Global Lakes and Wetlands Database (GLWD v2)

Bernhard Lehner<sup>1</sup>, Mira Anand<sup>1</sup>, Etienne Fluet-Chouinard<sup>2</sup>, Florence Tan<sup>1,3</sup>, Filipe Aires<sup>4</sup>, George H. Allen<sup>5</sup>, Philippe Bousquet<sup>6</sup>, Josep G. Canadell<sup>7</sup>, Nick Davidson<sup>8,9</sup>, C. Max Finlayson<sup>9,10</sup>, Thomas Gumbrecht<sup>11</sup>, Lammert Hilarides<sup>12</sup>, Gustaf Hugelius<sup>13</sup>, Robert B. Jackson<sup>14</sup>, Maartje C. Korver<sup>1</sup>, Peter B. McIntyre<sup>15</sup>, Szabolcs Nagy<sup>12</sup>, David Olefeldt<sup>16</sup>, Tamlin M. Pavelsky<sup>17</sup>, Jean-Francois Pekel<sup>18</sup>, Benjamin Poulter<sup>19</sup>, Catherine Prigent<sup>4</sup>, Jida Wang<sup>20,21</sup>, Thomas A. Worthington<sup>22</sup>, Dai Yamazaki<sup>23</sup>, Michele Thieme<sup>24</sup>

<sup>1</sup> Department of Geography, McGill University, Montreal, Quebec H3A 0B9, Canada

<sup>2</sup> Earth System Science Division, Pacific Northwest National Laboratory, Richland, WA, USA

<sup>3</sup> Department of Earth and Environmental Sciences, KU Leuven, Leuven, Belgium

<sup>4</sup> Observatoire de Paris, LERMA, CNRS, France

<sup>5</sup> Department of Geosciences, Virginia Polytechnic Institute and State University, Blacksburg, VA, USA

<sup>6</sup> Laboratoire des Sciences du Climat et de l'Environnement, Université Paris-Saclay, CEA, CNRS, UVSQ, Gif sur Yvette, France

<sup>7</sup> Global Carbon Project, CSIRO Environment, Canberra, ACT 2601, Australia

<sup>8</sup> Nick Davidson Environmental, Queens House, Ford Street, Wigmore HR6 9UN, UK

<sup>9</sup> Gulbali Institute for Agriculture, Water & Environment, Charles Sturt University, Albury, NSW, Australia

<sup>10</sup> Centre for Ecosystem Science, School of Biological, Earth and Environmental Sciences, UNSW Sydney, Sydney, NSW, Australia

<sup>11</sup> Department of Physical Geography, Stockholm University, 10691 Stockholm, Sweden

<sup>12</sup> Wetlands International, 6700 AL Wageningen, The Netherlands

<sup>13</sup> Department of Physical Geography and Bolin Centre for Climate Research, Stockholm University, SE 106 91 Stockholm, Sweden

<sup>14</sup> Department of Earth System Science, Woods Institute for the Environment, and Precourt Institute for Energy, Stanford University, Stanford, CA

<sup>15</sup> Department of Natural Resources and the Environment, Cornell University, Ithaca, NY 14853

<sup>16</sup> Department of Renewable Resources, University of Alberta, Alberta T6G 2G7, Canada

<sup>17</sup> Department of Earth, Marine and Environmental Sciences, University of North Carolina, Chapel Hill, NC 27599, USA

<sup>18</sup> European Commission, Joint Research Centre (JRC) Ispra, Italy

<sup>19</sup> NASA Goddard Space Flight Center, Biospheric Sciences Lab., Greenbelt, MD 20771, USA

<sup>20</sup> Department of Geography and Geographic Information Science, University of Illinois Urbana-Champaign, Illinois 61801, USA

<sup>21</sup> Department of Geography and Geospatial Sciences, Kansas State University, Kansas 66506, USA

<sup>22</sup> Conservation Science Group, Department of Zoology, University of Cambridge, Cambridge, UK

<sup>23</sup> Institute of Industrial Science, The University of Tokyo, Tokyo, 153-8505, Japan

<sup>24</sup> World Wildlife Fund, Washington, DC, 20037, USA

Correspondence to: Bernhard Lehner ([bernhard.lehner@mcgill.ca](mailto:bernhard.lehner@mcgill.ca))

**Abstract.** In recognition of the importance of inland waters, numerous datasets mapping their extents, types, or changes have been created using sources ranging from historical wetland maps to real-time satellite remote sensing. However, differences in definitions and methods have led to spatial and typological inconsistencies among individual data sources,



confounding their complementary use and integration. The Global Lakes and Wetlands Database (GLWD), published in 2004, with its globally seamless gridded depiction of major vegetated and non-vegetated wetland classes, has emerged over the last decades as a foundational reference map that has advanced research and conservation planning addressing freshwater biodiversity, ecosystem services, greenhouse gas emissions, land surface processes, hydrology, and human health. Here, we present a new iteration of this map, termed GLWD version 2, generated by harmonizing the latest ground- and satellite-based data products into one single database. Following the same design principle as its predecessor, GLWD v2 aims to avoid double-counting of overlapping surface water features while differentiating between natural and non-natural lakes, rivers of multiple sizes, and several other wetland types. The classification of GLWD v2 incorporates information on seasonality (i.e., permanent vs. intermittent vs. ephemeral); inundation vs. saturation (i.e., flooding vs. waterlogged soils); vegetation cover (e.g., forested swamps vs. non-forested marshes); salinity (e.g., salt pans); natural vs. non-natural origins (e.g., rice paddies); and a stratification of landscape position and water source (e.g., riverine, lacustrine, palustrine, coastal/marine). GLWD v2 represents 33 wetland classes and—including all intermittent classes—depicts a maximum of 18.2 million km<sup>2</sup> of wetlands (13.4% of the global land area excluding Antarctica). The spatial extent of each class is provided as the fractional coverage within each grid cell at a resolution of 15 arc-seconds (approximately 500 m at the equator), with cell fractions derived from input data at resolutions as small as 10 m. The updated GLWD v2 offers an improved representation of inland surface water extents and their classification for contemporary conditions. Despite being a static map, it includes classes that denote intrinsic temporal dynamics. GLWD v2 is designed to facilitate large-scale hydrological, ecological, biogeochemical, and conservation applications, aiming to support the study and protection of wetland ecosystems around the world.

## 60 **1 Introduction**

Wetland ecosystems ranging from lakes and rivers to marshes, swamps, peatlands, mangroves, and numerous other wetland types are critically important for humans and Earth system processes. As key components of global hydrological and biogeochemical cycles and as habitats for biodiversity, they provide some of the most valuable ecosystem services to human society (Costanza 1998; Millennium Ecosystem Assessment 2005). Wetlands directly and indirectly influence many environmental and socio-economic systems through their carbon storage (e.g., Chmura et al., 2003; Duarte et al., 2005; Raymond et al., 2013; Hugelius et al., 2020); nutrient processing (e.g., Cheng et al., 2020); provision of water, food and other resources (e.g., Mitsch et al., 2015); biological productivity (e.g., Gibbs, 2000; Mitchell, 2013); flood and drought mitigation (e.g., Tallaksen & Van Lanen, 2004; Čížková et al., 2013; Junk et al., 2013); coastal protection (e.g., Gedan et al., 2011; Marois & Mitsch, 2015); and water quality regulation (e.g., Verhoeven & Setter, 2010).

70 Accurate and comprehensive maps of wetland ecosystems are fundamental to quantifying their role within the water, carbon, and nutrient cycles, to plan conservation and restoration actions, and to assess and manage human interactions and pressures (van Asselen et al., 2013; Qiu et al., 2021). Beyond knowledge of their areal extent, characteristics such as vegetation, hydrology, salinity, and connectivity are critical for distinguishing the roles and behaviors of different wetland types.



Consistent information across large scales is required to set a global baseline to contextualize long-term degradation of wetland ecosystems (Vörösmarty et al., 2010; Darrah et al., 2019; Murray et al., 2019) and forecasted risks from climate change (e.g., Xi et al., 2021). While freshwater biodiversity is among the most threatened in the world (Ramsar Convention on Wetlands, 2021), several regions or countries have nearly eradicated their wetland cover since pre-industrial times (Fluet-Chouinard et al., 2023). Reliable maps are also needed for monitoring the progress towards global targets, such as to track changes in the extent of water-related ecosystems over time as mandated by the UN's Sustainable Development Goal 6.6 ("Protect and restore water-related ecosystems, including mountains, forests, wetlands, rivers, aquifers and lakes").

Global maps of inland (non-marine) wetland ecosystems have improved continuously over the last four decades (Figure 1). Literature estimates of global wetland extents range broadly from 5 to 13 million km<sup>2</sup>, with lower and upper boundaries of 2 and 17 million km<sup>2</sup> (Lieth, 1975; Matthews & Fung, 1987; Aselmann & Crutzen, 1989; Finlayson & Davidson, 1999; Spiers, 1999, 2001; Lehner & Döll, 2004; Prigent et al., 2007; Fluet-Chouinard et al., 2015; Mitsch & Gosselink, 2015; Tiner, 2015). The wide range is explained by differences in data sources, methodologies, and definitions. Early wetland estimates inherited gaps and inconsistencies from the compilation of national or regional inventories, limiting the reliability of their global perspective (Nivet & Frazier, 2004; Davidson et al., 2018). Over time, compilations of paper maps were replaced by satellite remote sensing imagery and its interpretation using machine learning and artificial intelligence which allowed for seamless mapping across the world at shorter time intervals (Gallant, 2015). These improvements in methods coincided with an increase of the global area of wetland ecosystems mapped over time (Davidson et al., 2018). Nonetheless, wetlands remain the land cover class with the least agreement when comparing across global data products, in which wetlands are often being misclassified as forest, shrub, cropland, or grassland (Nakaegawa, 2012). Even advanced remote sensing methodologies and sensors face challenges in detecting different wetland types or delineating the hydrologically active extent of wetlands, for example when cloud or vegetation cover obstructs the view or when saturated soils are confused with surface inundation (Gallant, 2015). Besides restrictions in spatial and/or temporal resolution, remote sensing approaches are also constrained by their limited historical extent as the first missions launched only in the 1970s.

Differences in definitions of what constitutes an aquatic ecosystem or wetland are the primary factor impeding comparisons across estimates and data sources. The Ramsar Convention on Wetlands (1971) adopted a broad definition of wetlands, comprising nearly all types of aquatic ecosystems as "*areas of marsh, fen, peatland or water, whether natural or artificial, permanent or temporary, with water that is static or flowing, fresh, brackish, or salt, including areas of marine water the depth of which at low tide does not exceed six meters.*" However, this definition is not universally accepted (Gerbeaux et al., 2016) and wetland criteria designed for field use are not practical for broad-scale mapping as shown by the wide range of areal estimates across studies (Mahdavi et al., 2018). Individual global map products typically provide their own, narrower definitions, justified by methodological limitations. For instance, inundation maps from passive microwave sensors may omit non-inundated peatlands and may require post-processing to exclude coastal and/or offshore ecosystems to avoid issues of signal oversaturation (Aires et al., 2017; Prigent et al., 2020). Similarly, a specific wetland definition may be required for different applications. For example, ecosystem conservation planning may exclude artificial wetlands such as rice paddies



(Reis et al., 2017); or estimates of methane emissions from wetlands may separate open waterbodies from vegetated wetlands to partition the emission budget (Saunois et al., 2020; Zhang et al., 2021) or to remove coastal regions because  
110 salinity inhibits methane production (Melton et al., 2013; Poffenbarger, 2011).

Some wetland ecosystem types and extents are better captured by current remote sensing capabilities than others. The distinction of open waterbodies from other wetland ecosystems has become easier with the advent of global river, lake, and other permanent water coverages derived from optical remote sensing (Pekel et al., 2016; Allen & Pavelsky, 2018; Pickens et al., 2020). However, seasonal fluctuations in inundation caused by changes in vegetation and/or saturated soils are not as  
115 reliably mapped and contribute disproportionately to the large uncertainties in global wetland estimates (Gallant, 2015). For instance, decadal-long observations estimate that the annual minimum and maximum global inundated areas vary by a factor of 2.8 (Prigent et al., 2007; Fluet-Chouinard et al., 2015). In contrast, some static wetland maps may represent average or maximum conditions, concealing major seasonal or interannual variation in inundation patterns (Prigent & Papa, 2015). Depending on the observation period and the definitions and methods used, different estimates of wetland ecosystems may  
120 prove to be complementary, overlap partially, or disagree entirely, thereby further complicating attempts to achieve a comprehensive view across all wetland ecosystem types.

To address the issue of spatial inconsistency, Lehner & Döll (2004) produced the Global Lakes and Wetlands Database (GLWD, hereon GLWD v1) by compiling and harmonizing existing wetland datasets into a single, coherent global database that distinguishes 12 types of waterbodies and wetlands. As one of the most comprehensive global wetland datasets  
125 (Nakaegawa, 2012; Mitsch & Gosselink, 2015), GLWD v1 facilitated the integration of wetlands into a broad range of large-scale land surface studies, and it remains one of the most widely used global wetland map to date (Lindersson et al., 2020). However, GLWD v1 has several limitations and drawbacks, including its coarse spatial resolution, outdated sources, the omission of small lakes and rivers, inaccuracies due to projection or generalization issues, and ambiguous definitions of wetland classes (Lehner & Döll, 2004). Since the publication of GLWD v1, newer maps of specific waterbody and wetland  
130 types have surpassed single classes of GLWD v1 in their accuracy and spatial or temporal resolution due to improved sensors and algorithms, longer archives, and refined training data (Figure 1). Despite these advances on individual waterbody and wetland types, GLWD v1 has not yet been replaced by a harmonized representation of the full range of inland wetland ecosystems. Consequently, the limitations of GLWD v1 described above still constrain scientific and management applications that require detailed knowledge of the global distribution of waterbodies and wetland types.

135

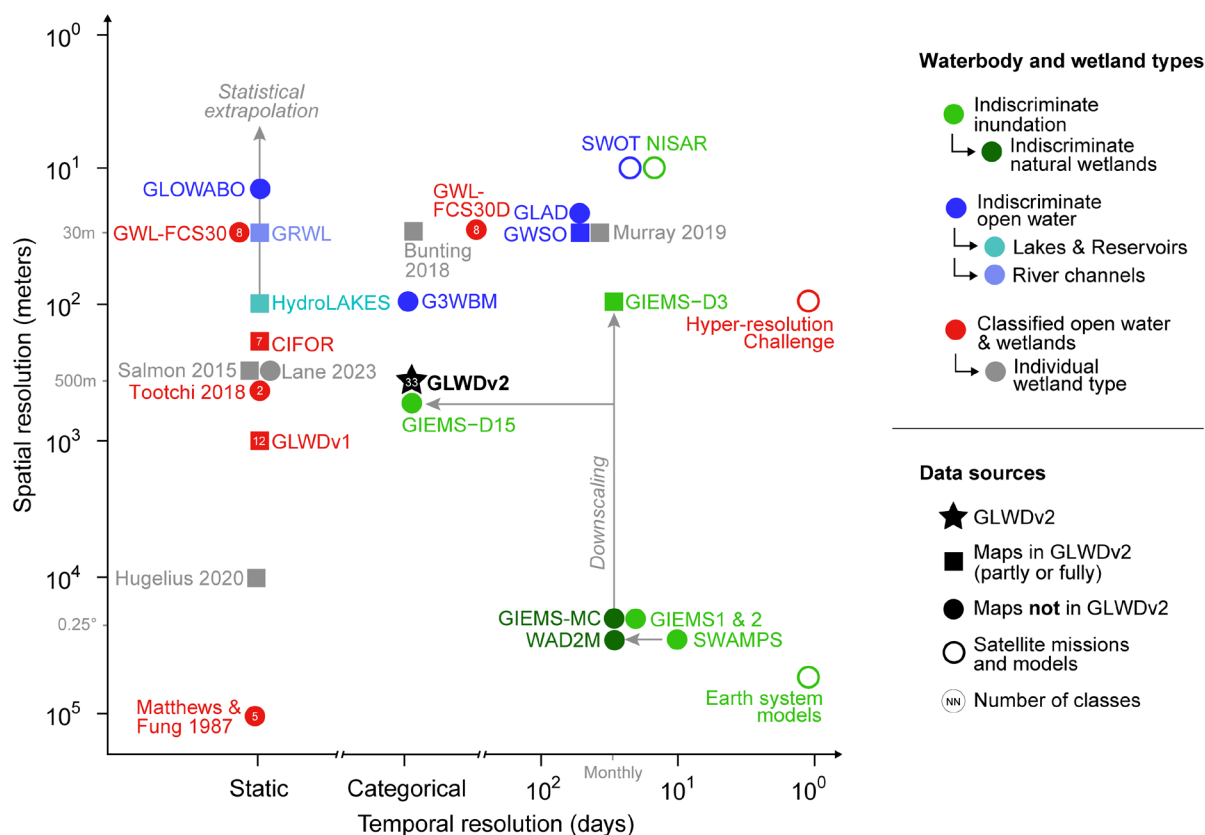


**Figure 1: Common surface water datasets plotted according to their spatial and temporal resolution. Only maps with global or near coverage, covering >80° of latitudinal swaths, are included. The colors of points represent the typological level of each dataset and together illustrate that classified maps including multiple wetlands and waterbody types have largely remained at a coarser resolution than available data products of indiscriminate wetland types. Arrows in the plot represent which datasets have been used in the production of others. Square points represent data products that were included in the creation of GLWD v2 as presented in this paper (additional detail on these sources can be found in Table 1). The spatial resolution is in meters at the equator. Data products described as ‘static’ do not describe flooding frequency, while data products depicting hydrological regimes with qualitative measures are labelled ‘categorical’. References for data sources are as follows: G3WBM: Yamazaki et al., 2015; GIEMS1: Prigent et al., 2007; GIEMS2: Prigent et al., 2020; GIEMS-D3: Aires et al., 2017; GIEMS-D15: Fluet-Chouinard et al., 2015; GIEMS-MC: Bernard et al., in prep.; GLAD: Pickens et al., 2020; GLOWABO: Verpoorter et al., 2014; GLWDv1: Lehner & Döll, 2004; GRWL: Allen & Pavelsky, 2018; GWL-FCS30: Zhang et al., 2023; GWL-FCS30D: Zhang et al., 2024; GWSO: Pekel et al., 2016; HydroLAKES: Messenger et al., 2016; SWAMPS: Jensen & McDonald, 2019; WAD2M: Zhang et al., 2021.**



Here, we introduce the Global Lakes and Wetlands Database version 2 (GLWD v2) which follows the same design principles as GLWD v1 and is intended to succeed it. GLWD v2 draws upon the best available free data sources to provide a comprehensive and seamless global map of inland surface waters distinguished into 33 non-overlapping waterbody and wetland types. To avoid double-counting across multiple sources and classes, we harmonized input sources at their finest resolution (see Methods) and aggregated the results to a common grid at 15 arc-second resolution (approximately 500 m at the equator). Beyond higher quality inputs and a higher spatial resolution, GLWD v2 features a key structural improvement over its predecessor in that it provides fractional cell coverage of wetland extents per class, rather than a single majority class per cell. This creates two important advantages, namely that 1) multiple classes can share the same grid cell (while the sum of all classes is constrained to not exceed full cell coverage); and 2) individual class layers can preserve wetland extents from original sources at sub-cell resolution without information loss, i.e., the cell's fractional wetland coverage can be calculated from fine-scale maps at resolutions as small as 10 m, where available. The classification of GLWD v2 follows a multi-factor hierarchical system, such that most classes can be grouped with others according to multiple criteria, including landscape position (inland vs. coastal/marine), water source (lacustrine vs. riverine vs. palustrine), vegetation (forested vs. non-forested), and soil type (mineral vs. organic). Finally, all 33 individual class maps were combined into one additional majority map to identify the dominant waterbody or wetland type in each grid cell, akin to the original map of GLWD v1. While GLWD v2 represents maximum extents of wetland ecosystems as a static map over the broad contemporary period of 1984-2020 as a static map, it also provides a simple depiction of intrinsic hydrological dynamics and variability through its classification (permanent, regular, seasonal, and ephemeral). With these numerous improvements, GLWD v2 offers a detailed baseline map of inland surface waters in preparation for time-resolved monitoring of the world's wetland ecosystems in the future.

## 2 Definitions and data sources

### 2.1 Wetland versus waterbody definitions

The working definition of wetlands and waterbodies as applied in GLWD v2 arises from the objective of being all-inclusive, and from practical considerations stemming from the fact that GLWD v2 inherits, at least in part, given definitions from its source datasets by association. As a result, the overarching wetland definition of GLWD v2 does not follow pre-established criteria but is nested within the broader perspective of the Ramsar Convention on Wetlands (1971; see Introduction) in that it includes all inland surfaces that are flooded or saturated longer than a certain period. However, a few Ramsar wetland types are excluded from GLWD v2: subtidal and offshore marine wetlands (e.g., coral reefs, kelp forests) because they lie outside the continental land surface; subterranean, karst and cave environments; as well as subglacial lakes (in part as Antarctica was excluded from the mapping efforts, see Methods).





To simplify the terminology, we here refer to the entire surface water extent covered by GLWD v2 as ‘wetland’, and in the context of GLWD v2 we consider ‘wetlands’, ‘aquatic environments’, and ‘inland/terrestrial surface waters’ as equivalent. We then use ‘waterbody’ to designate all standing or flowing open water surfaces of any size, typically detectable by optical remote sensing, regardless of whether the water is fresh, brackish, or salty, or whether the waterbody is of natural or human-made origin (e.g., reservoirs). Most but not all waterbodies have permanent open water, while some are intermittent. We use ‘other wetlands’ to refer more narrowly to all types of emergent and bare wetlands beyond waterbodies, whether inundated or saturated, permanent or seasonal, fresh, brackish, or salty, vegetated or non-vegetated, natural or human-made (e.g., rice paddies). We acknowledge that the name Global Lakes and Wetlands Database is not entirely consistent with this working definition, but we chose to retain it for historical continuity.

Wetlands are separated into 26 classes from a combination of biotic, geomorphic and hydrologic factors similar to the Ramsar system (Figure 2). Waterbodies in GLWD v2 are divided into 7 types aligning closely with Ramsar classes, although ignoring lake size as a criterion. Moreover, all 26 wetland ecosystem types in GLWD v2 can be grouped into five higher-level categories following the Cowardin system (Cowardin et al., 1979) on which Ramsar’s is based: lacustrine (lake-associated; lentic); riverine (river-associated; lotic); estuarine (river-associated; tidal); palustrine (depressional; isolated); and coastal (marine; tidal). Furthermore, the classification of wetland types in GLWD v2 adds elements of a hydrological wetland definition (temporal inundation dynamics and connectivity) as well as soil and vegetation characteristics.

## 2.2 Data sources, characteristics, and resolution

GLWD v2 was produced by fusing 25 primarily global datasets (Table 1) ranging from broad representations of wetland ecosystems (e.g., all inundated surfaces) to individual types (e.g., mangroves) and ancillary information (e.g., forest cover). The selection of these input datasets was made to a) avoid duplication of information by choosing the single most complete dataset per type based on criteria described below (e.g., only one lake dataset), and b) include only data with unrestricted use permissions so that GLWD v2 can be released with a free and open data license. Dataset characteristics and minimum requirements included globally consistent coverage, spatially uniform quality, sufficiently high spatial resolution (grid cell sizes mostly between 30 m and 500 m, or equivalent for vector layers), and proper documentation. The selection of some datasets was done for coherency with other inputs, for instance a shared shoreline delineation for freshwater lakes, saline lakes, and reservoirs. Data sources representing narrower types of waterbodies or wetlands were preferred over more general sources in order for GLWD v2 to depict wetland types in as much detail as possible.

Our approach of selecting the single best data source when multiple candidates exist for the same feature type suffers from the disadvantage of inheriting all of the source’s inaccuracies and uncertainties while precluding the potential benefits of correcting systematic deficiencies by compositing multiple datasets (e.g., filling gaps from cloud, snow or vegetation cover, or improving limited detection of small objects). However, we opted not to combine multiple datasets of the same feature type because of the inherent risks of duplication, distortion, and bias arising from the merger, in particular for inputs



215 capturing different time periods (e.g., shifting river meanders). Some exceptions were made to augment incomplete information in cases where regional datasets were combined (see Methods).

Applying data fusion procedures at high spatial resolution allows to identify coinciding water features which reduces the risk of double-counting in areas of overlap, yet the accuracy of each source dataset also determines the efficacy of the merger. The initial grid cell resolution of all processing steps for waterbody datasets (and certain wetland types, such as mangroves) was 1 arc-second (~30 m at the equator), reflecting the original resolution of most input datasets. Some preprocessing steps, such as reprojection and resampling, were conducted at even higher resolutions (3 m to 10 m) to minimize loss of information (see Methods). Other wetland types were processed at their respective native resolutions ranging from the highest resolution of ~10 m for saltmarshes to the coarsest dataset of ~1 km for saline/brackish wetlands; the latter requiring disaggregation. All input datasets were ultimately converted to the GLWD v2 target resolution of 15 arc-seconds (~500 m) and were expressed as fractional cell coverage to retain maximum information. Throughout all processing steps it was ensured that combined waterbody and wetland extents of all classes cannot exceed 100% in a single output grid cell.

**Table 1: Source datasets used for the creation of GLWD v2.**

Feature	Dataset/Source	Contents/Description	In GLWD v2
Lakes	HydroLAKES <i>Messenger et al., 2016</i>	Vector polygons of 1.4 million lakes, regulated lakes, and reservoirs $\geq 10$ ha. Saline lakes determined using methods by Ding et al. (2024).	Freshwater lakes and saline lakes
Reservoirs	Global Dam Watch Database <i>Lehner et al., in review</i>	Combined database of 35,295 reservoir polygons created by merging existing global datasets and manual curation.	Reservoirs
Rivers	Global River Width from Landsat (GRWL) Database <i>Allen &amp; Pavelsky, 2018</i>	30 m resolution raster product derived from Landsat imagery; supervised detection and classification of large rivers and estuarine rivers of widths $>90$ m.	Large rivers and estuarine rivers
Rivers	SWOT River Database (SWORD) <i>Atenau et al., 2021</i>	Vector product of center lines of large rivers for use by the Surface Water and Ocean Topography (SWOT) satellite mission.	Augmentation of large rivers
Rivers	RiverATLAS as part of HydroATLAS database <i>Linke et al., 2019</i>	Vectorized line network of all global rivers that have a catchment area of at least 10 km <sup>2</sup> or an average river flow of at least 0.1 m <sup>3</sup> /sec; extracted from the gridded HydroSHEDS layers at 500 m resolution.	Small streams
Open water	Global Surface Water (GSW) dataset by European Commission's Joint Research Center; <i>Pekel et al., 2016</i>	30 m (0.9 arc-second) resolution raster product from Landsat providing maps of global surface water from 1984 to present; water presence/absence (incl. maximum extent, recurrence); detects visible open water but contains omissions, e.g., due to cloud or vegetation cover.	Permanent, seasonal, ephemeral open water
Mangroves	Global Mangrove Watch 3.0 <i>Bunting et al., 2022</i>	0.8 arc-second resolution mangrove classification from SAR and Landsat data; baseline classification was expanded into a time-series of mangrove change using SAR data from 1996-2020.	Mangroves
Saltmarshes	Global tidal marshes 2020 dataset (version 2.6) <i>Worthington et al., 2024</i>	Spatial distribution of tidal marshes between 60°N to 60°S at 10 m grid cell resolution, derived using a random forest classification model applied to earth observation data from the year 2020.	Saltmarshes
Saltmarshes	Global Distribution of Saltmarshes (by UNEP) <i>Mcowen et al., 2017</i>	Polygons of saltmarshes across 99 countries, synthesized from a range of national and local datasets (points were not included in GLWD v2). Lacks data in some regions, e.g., Canada and northern Russia.	Saltmarshes
Intertidal areas	Tidal wetland probability <i>Murray et al., 2022</i>	30 m raster product predicting probability of tidal wetlands based on Landsat data and machine learning. Excludes areas north of 60°N.	Other coastal wetlands
Peatlands	PEATMAP <i>Xu et al., 2018</i>	Global meta-analysis polygon product which synthesizes national and regional peatland maps of varying source resolutions and quality.	Composite peatlands
Peatlands	SoilGrids250m <i>Hengl et al., 2017</i>	250 m resolution raster product of soil properties at multiple depths based on machine learning; peatland extents can be approximated by the histel (TAXOUSA) and histosol (HISTPR) soil layers.	Composite peatlands





Feature	Dataset/Source	Contents/Description	In GLWD v2
Peatlands	Northern peatland extents <i>Hugelius &amp; Oelefeldt, unpublished</i>	500 m grid showing percent probability of peatlands in northern regions (above 23°N) created by merging 2013 versions of soil grids, northern & mid-latitude soil databases, and others.	Composite peatlands
Wetlands	Global Wetlands Map (CIFOR) <i>Gumbricht et al., 2017</i>	250 m raster product of wetland classes and peatland depth in the tropics and subtropics (south of 40°N) based on an expert system.	Composite peatlands
Wetlands	GLWD v1 <i>Lehner &amp; Döll, 2004</i>	1 km global raster with 12 wetland classes produced from merged regional data, including class 'salt pan, saline/brackish wetland'.	Salt pan, saline/brackish wetlands
Inundated areas	GIEMS-D3 (Global Inundation Extent from Multi-Satellites) <i>Aires et al., 2017</i>	Downscaled 90 m raster product of inundation frequency (version 2 as of 2022) derived from 1993-2007 time series from multi-sensor remote sensing imagery; includes saturated soils and areas with vegetation.	Indiscriminate inundation surface
Floodplains	CaMa-Flood model results <i>Yamazaki et al., 2011</i>	CaMa-Flood model simulates floodplain inundation dynamics using a river-routing model with floodplain topography at 90 m (3 arc-second) resolution; data include flood probability over the period of 2001-2014.	Flooding classes and frequencies
Paddy rice	GRIPC (Global Rain-fed, Irrigated, and Paddy Croplands) <i>Salmon et al., 2015</i>	500 m global raster product developed from remote sensing imagery, climate data, and national and sub-national agricultural inventory data; contains classes of rain-fed, irrigated, and paddy cropland.	Paddy rice
Paddy rice	RiceAtlas <i>Laborte et al., 2017</i>	RiceAtlas (including RiceCalendar v1) shows the seasonal distribution of the world's rice-producing areas and countries in polygon units.	Correction of paddy rice
Deltas	Deltas at Risk <i>Tessler et al. 2015</i>	Compilation of 48 large river deltas from around the world as boundary polygons.	Delta classification
Forests	Global Forest Change map <i>Hansen et al., 2013</i>	30 m (0.9 arc-second) resolution map of forest extent (percent forest cover) and change from 2000-2022 derived from Landsat imagery.	Separation of non-forest vs. forest
Climate	World Climate Regions <i>Sayre et al., 2020</i>	Raster map of 18 climate regions at 250 m resolution, derived by combining global temperature and global moisture datasets.	Climate separation of peatland classes
Discharge	RiverATLAS <i>Linke et al., 2019</i>	RiverATLAS includes an associated global grid at 500 m resolution representing long-term (1971-2000) average discharge estimates.	Source of riverine classes
Glaciers	GLIMS (Global Land Ice Measurements from Space) <i>Raup et al., 2007</i>	Global polygon map of glacier extents.	Masking of glaciers
Urban areas	WSF (World Settlement Footprint) 2019 <i>Marconcini et al., 2020</i>	10 m resolution binary map showing the presence of human settlements derived from Sentinel-1 and Sentinel-2 data for 2019.	Masking of urban areas

## 230 3 Methods

### 3.1 Overview of methodology

The guiding principle for creating GLWD v2 was to consolidate and harmonize—without duplication—all input data sources to produce a versatile global map of wetland types that is useable in a broad spectrum of applications. Antarctica was excluded from the mapping efforts due to generally incomplete or unreliable spatial input data. Results are provided as a series of grids with a target cell size of 15 arc-seconds (~500 m) which was chosen as a compromise between the spatial resolution of existing input data sources, computing demands, and ease of use for global applications. It is important to note, however, that the information from finer resolution input data, including permanent water surfaces at ~30 m and saltmarshes at ~10 m resolution, is preserved in the fractional cell coverage of each wetland type. The classification scheme of GLWD v2 (Figure 2) is designed to be manageable (i.e., limited to a reasonable number of classes), expert guided rather than statistically derived, and representative of the needs of various research fields and disciplines. Each of the 33 wetland classes is provided as an individual global map depicting the extent of the respective class as cell fractions. The 33 maps are then combined to derive the total global wetland extent and to identify the dominant wetland class per grid cell.



The main processing steps of GLWD v2 are outlined in Figure 3 and are described in more detail in sections 3.2 to 3.5. The central procedure combines four types of data: a) high-resolution data of waterbodies; b) data of various resolutions of other wetland types; c) high-resolution downscaled or modeled data of indiscriminate inundated areas; and d) ancillary data to support the classification of indiscriminate wetland types and the refinement of classes.

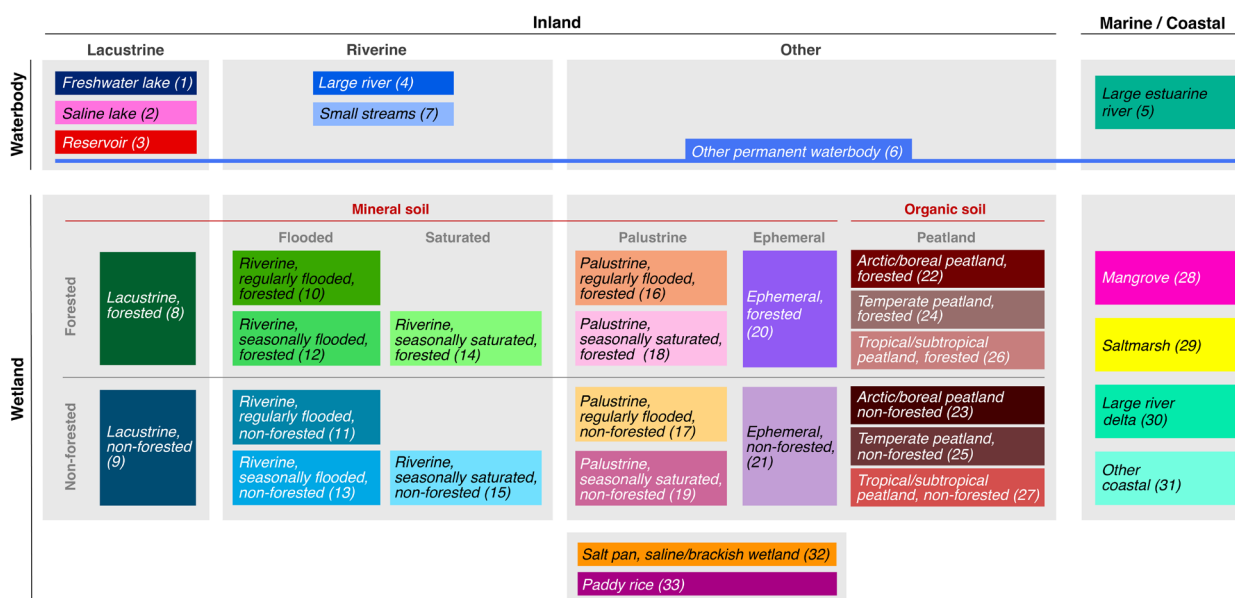
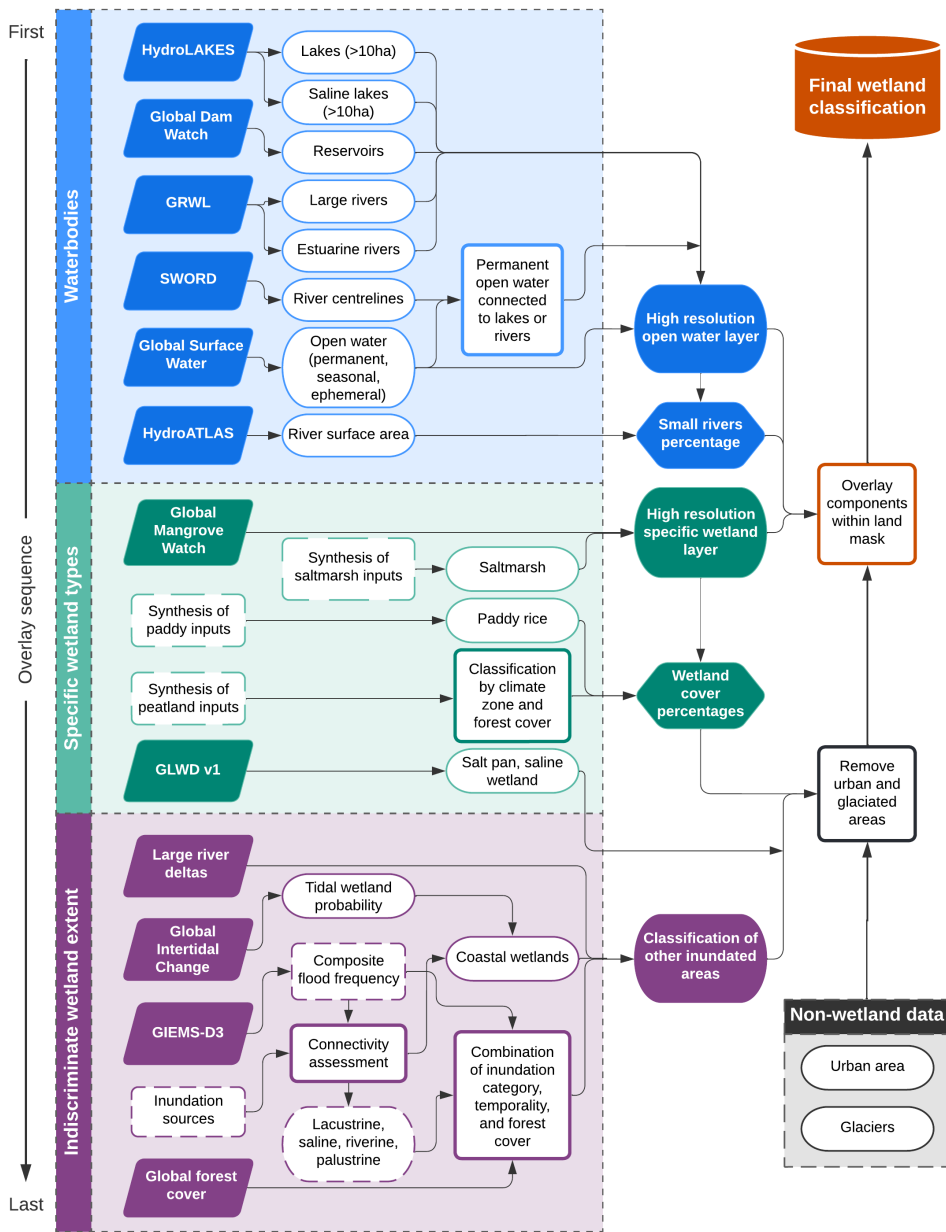


Figure 2: Schematic of classification hierarchy and distinctions among the 33 classes represented in GLWD v2. At the highest level, classes are grouped into 4 realms resulting from the 2x2 combinations of the overarching wetland division (*Waterbody vs. Other wetland [including emergent and bare wetlands]*) with landscape position (*Inland vs. Marine/Coastal*). Inland waterbodies and wetlands are then further divided according to water source and dynamic (*Lacustrine [lentic], Riverine [lotic], and Other [including Palustrine and Peatland]*). Other characteristics, such as soil type (*Mineral vs. Organic*) and vegetation cover (*Forested vs. Non-forested*) can be used to regroup wetland classes across water sources. Finally, mineral wetlands are further separated by their hydrological conditions (*Flooded vs. Saturated*) and regimes (*Ephemeral*).

For the merger, higher quality data sources were assigned priority over lower quality ones based on reliability, precision, resolution, confidence, completeness (in time and space), coherence, and information content (e.g., classified vs. unclassified data). When these criteria were ambiguous or conflicting (e.g., higher resolution but lower confidence), the prioritization of input datasets was guided by expert decision. The sequential merger of data layers was performed by a process we hereafter refer to as “inserting” wetland extents, whereby the next lower priority layer is successively allowed to occupy the grid cell space that remains free after all higher priority waterbodies and wetlands have been processed (analogous to ‘mosaicking’ in



GIS terminology). Data sources representing waterbodies were first combined following the order: lakes > reservoirs > rivers  
 265 > other subclasses. Next, data sources depicting individual wetland types were inserted around the waterbodies, followed by indiscriminate inundated areas that were subsequently classified using ancillary information. Thus, predominantly permanent waterbodies were spatially allocated first, and mostly non-permanent wetland extents were inserted thereafter to complement and surround these waterbodies. Finally, the map was refined by masking urban (built-up) and glaciated areas.



270



**Figure 3: Schematic of the workflow and main processing steps to create GLWD v2. This schematic broadly indicates the sequential order of insertion of different datasets, however some wetland types are reclassified or grouped together to produce the final set of 33 classes, as detailed in sections 3.2 - 3.4.**

275 The sequential merger of multiple layers of different original resolution to a common grid results in a mosaic where multiple wetland types can overlap in a 15 arc-second output cell, yet the sequence of layer stacking allows to subtract higher level features from lower level ones. This eliminates or at least reduces (depending on spatial precision and resolution of sources) double-counting in cases of spatial overlap and ensures that the summed waterbody and wetland coverage is bounded by the total area of each output cell.

## 280 3.2 Processing of waterbodies

The input datasets of waterbodies were processed globally at 1 arc-second (~30 m) resolution, except for small streams which were processed at 15 arc-second (~500 m) resolution. Some preprocessing steps were executed at higher resolutions (see details below). All data sources are listed in Table 1.

### 3.2.1 Lakes, saline lakes, and reservoirs

285 Lakes were extracted from the polygons of the HydroLAKES database (Messenger et al., 2016), which contains ~1.4 million lakes globally that are at least 10 ha in size. We converted the lakes of HydroLAKES v1.1 (including regulated lakes but excluding reservoirs) to a raster layer at 1 arc-second resolution according to whether at least half of each grid cell area was covered by a lake polygon. Reservoirs were extracted from the Global Dam Watch (GDW) database v1.0 (Lehner et al., in review), which contains >35,000 reservoir polygons globally, applying the same polygon to raster conversion as for lakes. It  
290 should be noted that HydroLAKES and the GDW database are spatially complementary and thus do not include any overlapping polygons.

Furthermore, we distinguished saline lakes (assuming a relatively high salinity threshold of 30 ppt, i.e., 30 g L<sup>-1</sup>) using a classification framework based on hydrography datasets, satellite imagery, and literature documentation as described in Ding et al. (2024). The supervised classification identified a total of 24,374 saline lakes, mostly located in endorheic (closed)  
295 inland depressions and arid or semi-arid climate zones. These conditions are conducive to salinity accumulation due to lack of surface outflow, strong potential evaporation, or both. Many of the detected saline lakes exhibit lacustrine evaporites visible from satellite images. To evaluate the overall robustness of the classification method, we conducted an independent literature search for all lakes exceeding 500 km<sup>2</sup> in surface area which confirmed that all 66 reported saline lakes (with salinity levels exceeding 3 g L<sup>-1</sup>) in that size class were correctly detected in the supervised classification, and only one  
300 saline lake from the supervised classification required conversion to non-saline.



### 3.2.2 Rivers and estuarine rivers

Rivers and estuarine rivers were extracted from the raster layers of the Global River Width from Landsat (GRWL) Database (Allen & Pavelsky, 2018). It should be noted that the original GRWL data also offer a ‘lake’ class, but we used this class only as a component layer to identify and conserve critical connections between lakes and their in- or out-flowing river courses. After Step 3.2.3 below, the ‘lake’ class from GRWL was discarded to avoid double-counting of lakes.

We reprojected and resampled all published 10×10 degree GRWL tiles from their original 30 m resolution and UTM projection to match the geographic coordinate system of GLWD v2 at a 0.25 arc-second (~8 m) resolution. This high-resolution version was then aggregated and mosaicked to create a seamless global layer that retained all 1 arc-second cells with at least 50% river coverage. The GRWL tiles can exhibit minor gaps at their edges when combined into a seamless global coverage, which we rectified by inserting data inside a 0.1-degree buffer around all edges from an unpublished version of GRWL (provided by the authors) of slightly inferior quality but with overlapping tiles.

To further ensure connectivity between river surfaces and adjacent lakes in the subsequent combination steps, we also processed and inserted the related vector product of the Surface Water and Ocean Topography (SWOT) River Database (SWORD) (Altenau et al., 2021) which presents center lines for all GRWL rivers including their paths traversing through lakes. We converted these vector lines to a grid at 1 arc-second resolution, added a one-cell buffer to produce slightly wider river lines, and retained only those SWORD cells that coincided with a GRWL ‘lake’. Furthermore, as the SWORD river center lines can cross land, such as over islands within a braided river system, we removed all SWORD river cells farther than one cell from the permanent open water class of the Global Surface Water (GSW) dataset (see next step).

### 3.2.3 Other permanent waterbodies

We used the Global Surface Water (GSW) dataset (Pekel et al., 2016) to complement the lakes, reservoirs, and rivers. GSW offers gridded data at 0.9 arc-second resolution (~27 m) compiled from Landsat imagery spanning the years 1984 to present. We used the separation of GSW into permanent, seasonal, and ephemeral classes from its ‘transitions’ layer for the years 1984 to 2020 and resampled it to our target 1 arc-second resolution. Cells labeled as seasonal or ephemeral and coinciding with a GRWL ‘lake’ were reclassified as permanent to conserve the lake-river connections in subsequent steps. We then inserted permanent GSW cells as their own waterbody class in GLWD v2, which nominally includes but does not distinguish between small lakes, ponds, rivers, and canals that exceed the 27 m detection threshold of GSW and have not been depicted in any of the previous datasets. The seasonal and ephemeral classes were integrated into the broader wetland classification in subsequent steps (section 3.4).

### 3.2.4 Combination of waterbody classes and reclassification of some cells

We combined the open waterbody features at the 1 arc-second resolution described in the previous steps by overlaying them in the following priority order: freshwater lake > saline lake > reservoir > river > estuarine river > other permanent



waterbody. In instances where waterbody boundaries were misaligned in the source datasets (e.g., a lake from HydroLAKES may not cover the entire permanent water from GSW; or a gap exists between the outlines of hydrologically connected lakes and rivers), we reclassified some of the gap cells of GSW from ‘other permanent waterbody’ to the type of the adjacent  
335 waterbody. This reclassification was performed based on proximity along contiguous cells from the waterbodies up to a maximum distance of 0.002 degrees (~200 m).

### 3.2.5 Adding small streams

The surface extent of small rivers and streams is not well captured in global remote sensing imagery due to the narrow, linear features in sub-meter dimensions (Allen et al., 2018). To account for this omission, a statistical estimate of the surface area  
340 of small streams was produced using river area estimates from the RiverATLAS database (Linke et al., 2019), which in turn were derived from discharge estimates and simple hydraulic geometry laws (Allen et al., 1994). The total surface area of rivers and streams was calculated by multiplying the estimated channel width and length of every river reach that exceeds 10 km<sup>2</sup> in catchment area or 100 L s<sup>-1</sup> in average flow in each 15 arc-second grid cell (Linke et al., 2019). To represent only small streams and avoid double-counting with larger rivers already mapped by GRWL (Step 3.2.2), the GRWL river extent  
345 was subtracted from the total river area provided by RiverATLAS in each 15 arc-second cell. Given the uncertainty of this estimation method, small streams were given the lowest priority among all waterbodies. Finally, the maximum extent of small streams was limited to 10% of each 15 arc-second cell (~2.5 ha), which resembles a river reach of approximately 500 m length (one cell) and 50 m width, as the GRWL product should cover rivers exceeding this size, even if not coinciding within a given cell due to potential spatial mismatches. It should be noted that while ‘small streams’ are grouped within the  
350 waterbody classes of GLWD v2, 50-60% of small streams globally have been estimated to be intermittent or ephemeral (Messenger et al., 2021).

### 3.3 Processing of explicit wetland types

Datasets representing the distribution of explicit wetland types were processed globally at 0.3, 1, 3, or 15 arc-second resolution (~10, 30, 90, or 500 m, respectively) depending on their native data format. All data sources are listed in Table 1.

#### 355 3.3.1 Insertion of high-resolution coastal wetland classes

We used original high-resolution source data to define the extent of three explicit coastal wetland types at the target processing resolution of 1 arc-second (~30 m): mangroves (Bunting et al., 2022), saltmarshes (Worthington et al., 2024; Mcowen et al., 2017), and intertidal areas (Murray et al., 2022). The mangrove class was produced from the maximum mangrove extent in the source data after resampling from its original 0.8 arc-second resolution. The saltmarsh class was  
360 created by first resampling the original ~10 m resolution tiles of the dataset by Worthington et al. (2024) and converting all provided saltmarsh polygons of the dataset by Mcowen et al. (2017) to the target 1 arc-second resolution. Given the lower accuracy and completeness of the dataset by Mcowen et al. (2017), it was only inserted for regions north of 60° N where no





365 data from Worthington et al. (2024) existed. The intertidal wetland areas, which were later combined into the ‘other coastal wetland’ class, were resampled from their original ~30 m resolution and all grid cells with a given probability of inundation of at least 50% were retained. The three classes were then inserted into the map of harmonized waterbody classes (see Steps 3.2.1 to 3.2.5), giving priority to waterbodies followed by mangroves > saltmarshes > intertidal areas.

### 3.3.2 Masking of urban and glaciated areas

370 Up until this step, all previous data sources were included into GLWD v2 without further corrections because they met high standards of spatial accuracy and detail. Before adding coarser resolution information, however, high-resolution non-wetland masks for urban areas and glaciated areas were inserted at the 1 arc-second resolution to prevent subsequent steps from allocating wetlands to these surfaces. The urban areas were aggregated from the original 10 m resolution of the World Settlement Footprint 2019 binary mask (Marconcini et al., 2021) to produce a percentage cover at 1 arc-second resolution and cells with at least 50% settlement cover were classified as urban. Glaciated areas (Raup et al., 2007) were converted from their original polygon format to the target 1 arc-second resolution. At the end of all processing steps, the urban and 375 glaciated classes were discarded from the final GLWD v2 map.

### 3.3.3 Insertion of paddy rice class

Paddy rice extents (Salmon et al., 2015) were inserted as percent coverage into all remaining unoccupied areas. The original grid delineating paddy rice extents with a predictive model included numerous artifacts such as erroneous small patches over regions with no known rice production. Furthermore, under realistic conditions paddy rice typically forms only part of a 380 heterogeneous landscape mosaic, where rice fields intersperse with other agriculture, roads, and small settlements, i.e., at a 500 m resolution each grid cell is covered by less than 100% paddy rice. We therefore converted the paddy rice layer from its original binary format to a fractional 0-100% range using several preprocessing steps. After reprojecting and resampling the original data to the target geographic coordinate system and 15 arc-second cell resolution of GLWD v2, we calculated each 15 arc-second cell’s rice fraction as the percentage of the original paddy rice extent found within a distance of ~2 km 385 around the cell (using a 9×9 cell neighborhood). We then used the administrative areas available as part of the RiceAtlas (Rice Calendar v1; Laborte et al., 2017) to discard regions where no paddy rice production is reported (after some minor manual corrections). Finally, the maximum paddy rice extent within a grid cell was capped at 50% and any paddy rice coverage below 20% was considered an inherent data error (mostly occurring along marine coastlines) and was removed. These thresholds, besides delivering visually plausible paddy rice regions, were chosen in an iterative trial-and-error process 390 to approximately match the reported global paddy rice extent of ~1.2 million km<sup>2</sup>, as well as the reported extents of the two dominant paddy rice countries of India (~400,000 km<sup>2</sup>) and China (~250,000 km<sup>2</sup>) (see Table 4 in Results for sources).



### 3.3.4 Insertion of peatland classes

Several global or near-global peatland extent maps have been developed in the past, each with its own specificities, strengths, and weaknesses, which led us to conclude that no single data product is of sufficient quality and/or completeness to represent all peatlands in GLWD v2. Therefore, we created a new composite peatland probability map from four input datasets (Table 1): PEATMAP (Xu et al., 2018; global), SoilGrids250m (Hengl et al., 2017; global), Northern Peatlands (Hugelius & Olefeldt, unpublished; north of 23° N), and CIFOR (Gumbrecht et al., 2017; south of 40° N, of which we only used data south of 23.5° N). The four input datasets were first reprojected and/or resampled into the geographic coordinate system of GLWD v2 and converted to a peatland percentage cover in each 15 arc-second grid cell, as follows:

PEATMAP originally offers spatial peatland percentages for regions in Canada and some areas in eastern Asia (0-100%), and otherwise binary presence/absence information which we set to 100% and 0%, respectively. PEATMAP is provided in polygon format which we corrected for some slight locational misalignments across Oceania and some regions of East Asia. Also, individual polygon parts with an area <20 ha (i.e., smaller than one grid cell in our target 15 arc-second resolution) were removed as upon visual inspection many of them represented spurious outliers and artifacts rather than precise peatland boundaries. SoilGrids250m offers cumulative probabilities (0-100%) of histosols occurring in any 250 m grid cell globally, as well as an independent probability of histels. We used the maximum value of histosols or histels per 15 arc-second cell and interpreted the result as the spatial probability of peatland occurrence in percent. The Northern Peatlands grid is based on the same underpinning data and methods as presented in Olefeldt et al. (2021) and was re-produced here as a 15 arc-second grid specifically for the purpose of inclusion in GLWD v2. It offers percent peatland extent per grid cell for histosols and histels, separately, which we summed into one grid (0-100%). Finally, the CIFOR dataset includes a binary peatland classification which we interpreted as 0 or 100% coverage, respectively. Furthermore, to avoid abrupt spatial transitions in the binary information of CIFOR, we inserted the values from SoilGrids250m wherever CIFOR showed zero values.

After standardization, the four layers of peatland probabilities were combined into an equally-weighted average; i.e., by calculating the average of the respective three input grids that existed north of 23.5° N and south of 23° N; and the average of all four input grids in the 0.5° transition zone using an edge smoothing (blending) approach. Calculating averages ensures that final extent probabilities remain within 0 and 100% and that the total global peatland extent falls within the individual estimates of the input datasets. We removed values below 3% from the final composite peatland map as these low percentages occurred throughout the globe including in areas of no known peatland extent, mostly due to artefacts of low probabilities inherent in the SoilGrids250m product of histosols and histels.

To create three climatological peatland types, we combined the composite peatland map with reclassified climate zones from the World Climate Regions (Sayre et al., 2020) which we first resampled from the original ~250 m to 15 arc-second resolution. We separated peatlands into arctic/boreal (original polar and boreal climates), temperate (original cool and warm temperate climates), and tropical/subtropical (original tropical and subtropical climates); and we applied a manual adjustment in that arctic/boreal climates were reclassified to temperate in regions below 43° N (with some additional



425 adjustments of small non-contiguous areas between 43° N and 55° N) to avoid the occurrence of minor arctic/boreal  
peatlands within tropical/subtropical mountains.

Finally, each of the three peatland classes was further subdivided into forested vs. non-forested using the same ancillary  
forest data and approach as described in more detail in Step 3.4.3 below. The six resulting combinations of climatological  
and forested/non-forested peatland classes were then inserted into GLWD v2.

### 430 **3.3.5 Insertion of salt pan/saline/brackish class**

In the absence of better global information, the extent of salt pans and saline/brackish wetlands was taken from the gridded  
version of GLWD v1 and disaggregated from its original 30 to 15 arc-second resolution. The salt pans and saline/brackish  
wetlands were assumed to occupy 100% of the original grid cells. Before insertion into GLWD v2, this class was augmented  
with the saline class derived in Step 3.4.2 below. An exception to our fusion rules was made in that this class could later be  
435 replaced by the two wetland types ‘large river delta’ and ‘other coastal wetland’ (see section 3.4) as these two classes were  
considered more reliable than the coarse GLWD v1 product.

## **3.4 Processing and classification of indiscriminate wetland extents**

Datasets representing the distribution of indiscriminate wetland extents were processed globally at 3 arc-second (~90 m)  
resolution. First, an all-encompassing global inundation extent map was created, which was then classified using ancillary  
440 data and an analysis of connectivity to the nearest waterbody. All data sources are listed in Table 1.

### **3.4.1 Determination of maximum inundation extent and flood frequencies**

We created an indiscriminate maximum inundation extent map at 3 arc-second resolution and assigned flood frequency  
values to each cell by combining four input datasets: (1) the downscaled GIEMS-D3 inundation data at 3 arc-second  
resolution over 1993-2007 (Aires et al., 2017) which formed the majority of the maximum extent as it includes both  
445 permanent open water and temporary wetlands; (2) the waterbody layer of GLWD v2 produced in Steps 3.2.1 to 3.2.4 at 1  
arc-second resolution (i.e., without small streams); (3) the seasonal and ephemeral open water cells of the GSW datasets at 1  
arc-second resolution; and (4) the flooded extent simulated by the CaMa-Flood model as inundated for more than 7 days per  
year at 3 arc-second resolution (Yamazaki et al., 2011). The 1 arc-second input datasets were aggregated to 3 arc-second  
resolution by defining each 3 arc-second grid cell as inundated if it contained at least one wetland cell at 1 arc-second  
450 resolution.

All four inundation data sources were combined by extracting the maximum inundation frequency (0-100%) per grid cell  
among the sources. With its broad coverage, the GIEMS-D3 database provided most of the inundation frequency estimates  
(0-100%), but was supplanted by: GLWD v2 waterbodies (assumed to have 100% inundation frequency as most of these  
waterbodies are permanent); seasonal GSW cells (80%, broadly based on GSW statistics); CaMa-Flood inundation (10%,



455 slightly above the applied minimum inundation threshold of 7 days per year); or ephemeral GSW (5%, GSW statistics),  
wherever they occurred.

### 3.4.2 Division of indiscriminate inundation into broad categories using hydrological connectivity

In order to classify the wetlands encompassed by the indiscriminate inundation extent, we first stratified the maximum extent  
map (Step 3.4.1) into one of five broad water source categories: lacustrine, saline, riverine, coastal, and palustrine—to be  
460 further refined in later steps (Step 3.4.3). These five categories were derived by determining the nearest hydrologically  
connected flooding source (waterbody, ocean, or local runoff) for each indiscriminate inundation cell, with hydrologic  
connectivity and distances being measured along flow paths between contiguous wetland cells. The flooding sources for the  
five categories originated from the previously assigned GLWD v2 classes, such that: cells nearest to freshwater lakes or  
reservoirs were classified as lacustrine; cells nearest to saline lakes as saline; cells nearest to rivers as riverine; cells nearest  
465 to estuarine rivers or the ocean as coastal; and all other cells disconnected from a source as palustrine.

Several additional criteria were applied in the determination of connectivity and proximity, and all parameters and thresholds  
were set by expert visual judgment in known wetland complexes. We used the flood frequency map (Step 3.4.1) as input to  
trace paths of flooding between every inundated cell and its most likely source of flooding. The most plausible connectivity  
was determined through a custom algorithm which ensured that the shortest flow paths followed preferential flow directions  
470 from each cell towards the neighboring cell with highest flood frequency, while remaining within contiguous inundation  
cells. This approach permits cells to be assigned a more spatially distant source if the flood frequencies are higher along that  
path. The process development and thresholds of lacustrine and coastal source attribution (see above and below) were  
informed by visual comparison with the elevation range from variations in lake surface water elevation observed by ICESat-  
2 (Cooley et al., 2021) and along coastlines by a reanalysis of tides and surges (Muis et al., 2022).

475 Two iterations of the connectivity assessment were performed. First, connectivity along cells with flood frequencies  $\geq 80\%$   
was determined to represent more persistent inundation and direct connectivity of wetlands fringing their adjacent  
waterbodies. This iteration was assumed to fully define the lacustrine and saline categories and they were removed from the  
following iteration. Second, unassigned inundated cells were categorized into riverine and coastal with an expanded  
connectivity assessment over cells of  $>10\%$  inundation frequency and using previously assigned riverine and coastal cells as  
480 additional sources. Also, riverine sources were supplemented in the second iteration by cells with a long-term average  
discharge exceeding  $1000 \text{ L s}^{-1}$  from the RiverATLAS database (Linke et al., 2019). During both iterations, grid cells with an  
elevation above 10 m a.s.l. were excluded from becoming coastal. All grid cells without an assigned category after both  
iterations, signifying no surface hydrological connectivity to flooding sources, were labeled as palustrine.

### 3.4.3 Final classification of indiscriminate wetlands with ancillary data

485 The lacustrine, riverine, and palustrine categories were further subdivided into 14 classes based on flood frequencies and  
forest cover (Table 2). Due to the thresholds used in the previous step, the only category containing grid cells with flood



frequencies below 10% was palustrine. These palustrine wetlands with low-frequency flooding were further constrained to a minimum frequency of 3% to remove the highly uncertain representation of rarely inundated extents in GIEMS-D3 data, and then relabeled as ‘ephemeral’.

490 Forest cover (Hansen et al., 2013) was used to separate between wetlands that fit the general definition of forested swamps vs. non-forested freshwater marshes. For this process, the percent tree cover values were first resampled by averaging from the original 0.9 to 3 arc-second resolution. To also accommodate shrubbed swamps, we set a relatively low threshold of 10% tree coverage for forested wetlands, which was visually calibrated to match known swamp occurrences including parts of the Pantanal in South America; the Tonle Sap freshwater swamp forests in Asia; and the Sudd, Okavango, Bangweulu, and  
 495 Niger Delta swamps in Africa.

Large river deltas were discerned as an additional class within the indiscriminate inundation areas using ancillary information. We converted the polygons of large river deltas (Tessler et al., 2015) to a grid at 3 arc-second resolution, and because of their low-precision outlines we extended them with a ~1 km buffer (15 grid cells) to avoid spurious gaps at the land-ocean boundary. Finally, delta areas were clipped to the extent of the maximum inundation map (Step 3.4.1). The large  
 500 river delta class superseded all other classes of the indiscriminate inundation areas.

**Table 2: Lacustrine, riverine, and palustrine wetland types.**

GLWD v2 class	Category	Flood frequency	Forest cover
Lacustrine, forested	Lacustrine	≥80% recurrence on GIEMS-D3	≥10%
Lacustrine, non-forested		≥80% recurrence on GIEMS-D3	<10%
Riverine, regularly flooded, forested	Riverine	≥50% recurrence on GIEMS-D3	≥10%
Riverine, regularly flooded, non-forested		≥50% recurrence on GIEMS-D3	<10%
Riverine, seasonally flooded, forested		Flooded on CaMa-Flood	≥10%
Riverine, seasonally flooded, non-forested		Flooded on CaMa-Flood	<10%
Riverine, seasonally wet, forested		10-49% recurrence on GIEMS-D3, or seasonal on GSW	≥10%
Riverine, seasonally wet, non-forested		10-49% recurrence on GIEMS-D3, or seasonal on GSW	<10%
Palustrine, regularly flooded, forested	Palustrine	≥50% recurrence on GIEMS-D3	≥10%
Palustrine, regularly flooded, non-forested		≥50% recurrence on GIEMS-D3	<10%
Palustrine, seasonally wet, forested		10-49% recurrence on GIEMS-D3, or seasonal on GSW	≥10%
Palustrine, seasonally wet, non-forested		10-49% recurrence on GIEMS-D3, or seasonal on GSW	<10%
Ephemeral, forested	Palustrine	3-9% recurrence on GIEMS-D3, or ephemeral on GSW	≥10%
Ephemeral, non-forested		3-9% recurrence on GIEMS-D3, or ephemeral on GSW	<10%

### 3.4.4 Inserting all classified inundation extents

505 As a last step, all classified inundation extents from Steps 3.4.2 to 3.4.3 were inserted into GLWD v2. At this stage, we grouped a small number of conceptually similar classes to simplify and eliminate ambiguities: outside of large river deltas, the coastal wetland category was combined with the intertidal wetlands (Step 3.3.1) to form the ‘other coastal wetlands’ class; and the saline wetland category was added to the ‘salt pan, saline/brackish wetland’ class (Step 3.3.5). At the lowest hierarchy level, all lacustrine, riverine, and palustrine classes (Table 2) were inserted into GLWD v2.



### 510 3.5 Creation of final GLWD v2 maps

For each of the 33 GLWD v2 wetland classes, an individual global grid was produced at the output 15 arc-second resolution showing the percent coverage of the respective wetland class per grid cell. In addition, the resulting spatial extents of all wetland classes were summed for each cell, creating a total global wetland extent map (the maximum total extent was capped at 100% whenever rounding caused slight exceedances). These 34 maps were also produced as absolute areas (in ha) per grid cell—using geodesic calculations—for ease of application. Finally, the dominant wetland class per grid cell (i.e., the class showing the highest fractional wetland coverage per cell) was determined to create a single global map of wetland types.

## 4 Results

GLWD v2 distinguishes 7 waterbody types and 26 other wetland types for a total of 33 distinct non-overlapping classes (Table 3). It provides a static snapshot of the inland surface water extent and climatology for contemporary conditions, centered around the period 1984-2020 of most of its input data. Its nominal spatial resolution is 15 arc-seconds (~500 m), yet it provides cell fractions of wetland cover that are derived from water surfaces at resolutions as fine as 0.3 arc-seconds (~10 m) to preserve smaller waterbodies. This database surpasses its predecessor, GLWD v1 (Lehner & Döll, 2004) in detail, consistency, and comprehensiveness to serve a broad range of applications by offering a composite global map of wetland ecosystem types.

### 4.1 Global wetland extent

The total combined extent of all classes in GLWD v2 including all inland and coastal waterbodies and wetlands of all inundation frequencies—that is, the maximum extent—covers 18.2 million km<sup>2</sup>, equivalent to 13.4% of total global land area excluding Antarctica. Most wetlands are found in Asia (43.8% of global wetland extent) followed by North and Central America (26.7%) (Table 3), which generally agrees with the results from the compilation of multiple wetland inventories undertaken by Davidson et al. (2018). These two continents also show the highest wetland-to-land ratios (18.7% and 19.9%, respectively) while Africa and Oceania exhibit the lowest wetland ratios (5.3% and 6.5%, respectively). Regions with high densities of wetlands include South and Southeast Asia, in part due to large swaths of paddy rice fields, the tropics where large riverine complexes exist, and areas north of ~45° N where lakes and peatlands dominate the landscape (Figures 4 and 5). Overall, the patterns of global wetland distribution correspond closely with regional climatic, physiographic, and hydrologic conditions.

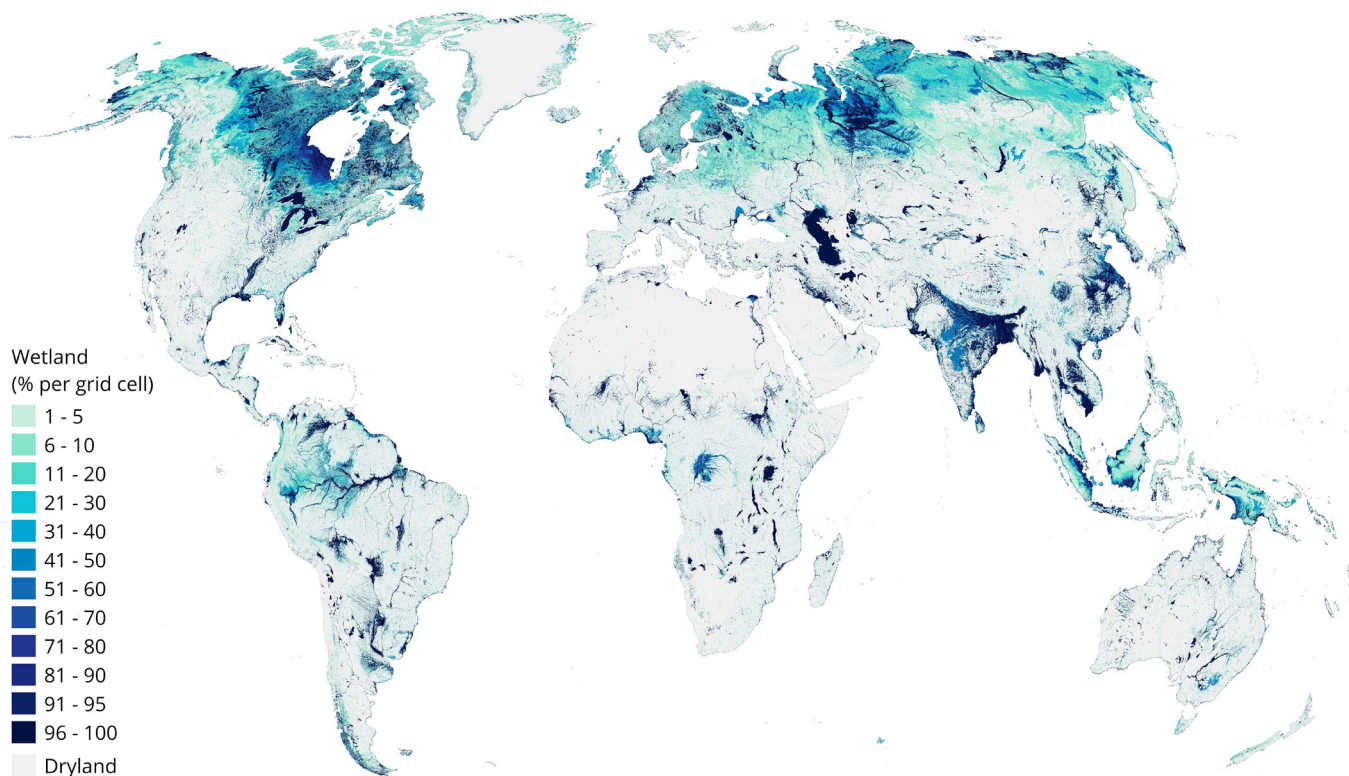




540

**Table 3: Continental and global extents of GLWD v2 wetland classes. Values in parentheses represent the continent's percent of the global extent of each class, except for two bottom rows which refer to all wetlands globally. Areas are in 10<sup>3</sup> km<sup>2</sup> except for totals in two bottom rows which are in 10<sup>6</sup> km<sup>2</sup>. Asia includes all of Russia; North America includes Greenland; Oceania includes Australia, New Zealand, Melanesia, Micronesia, and Polynesia; total land area excludes Antarctica.**

ID	Class Name	Continental area [10 <sup>3</sup> km <sup>2</sup> ]   (% of global class area)						Global class area	
		Africa	Asia	Europe & Middle East	North & Central America	South America	Oceania	Global class area [10 <sup>3</sup> km <sup>2</sup> ]	% of total wetland area
1	Freshwater lake	197.3 (9.6)	407.3 (19.9)	119.8 (5.8)	1226.6 (59.9)	83.3 (4.1)	13.8 (0.7)	2048.1	(11.3)
2	Saline lake	34.2 (5.1)	531.9 (79.7)	17.0 (2.6)	22.2 (3.3)	21.0 (3.2)	40.9 (6.1)	667.2	(3.7)
3	Reservoir	40.2 (12.7)	108.9 (34.5)	26.3 (8.3)	88.2 (28.0)	47.4 (15.0)	4.6 (1.5)	315.7	(1.7)
4	Large river	40.6 (10.6)	177.0 (46.2)	13.6 (3.6)	53.1 (13.9)	93.2 (24.3)	5.9 (1.5)	383.6	(2.1)
5	Large estuarine river	6.1 (7.8)	35.9 (45.7)	4.1 (5.2)	12.7 (16.1)	15.5 (19.7)	4.3 (5.5)	78.6	(0.4)
6	Other permanent waterbody	21.9 (3.6)	214.3 (35.3)	57.6 (9.5)	234.1 (38.5)	46.9 (7.7)	33.1 (5.4)	607.7	(3.3)
7	Small streams	20.9 (16.4)	45.6 (35.8)	9.4 (7.4)	21.9 (17.2)	24.1 (18.9)	5.4 (4.3)	127.2	(0.7)
8	Lacustrine, forested	19.6 (4.6)	67.8 (15.8)	28.6 (6.7)	261.3 (60.9)	49.7 (11.6)	1.7 (0.4)	428.8	(2.4)
9	Lacustrine, non-forested	21.0 (4.2)	154.5 (30.9)	27.6 (5.5)	235.4 (47.1)	55.5 (11.1)	5.6 (1.1)	499.6	(2.7)
10	Riverine, regularly flooded, forested	27.9 (7.4)	114.0 (30.1)	14.8 (3.9)	108.6 (28.7)	109.7 (29.0)	3.7 (1.0)	378.6	(2.1)
11	Riverine, regularly flooded, non-forested	31.2 (5.6)	299.8 (53.9)	35.2 (6.3)	121.3 (21.8)	64.0 (11.5)	4.6 (0.8)	556.3	(3.1)
12	Riverine, seasonally flooded, forested	220.3 (27.4)	157.9 (19.6)	15.7 (2.0)	79.1 (9.8)	311.3 (38.7)	20.9 (2.6)	805.2	(4.4)
13	Riverine, seasonally flooded, non-forested	202.4 (22.7)	323.2 (36.2)	93.1 (10.4)	63.0 (7.1)	114.9 (12.9)	96.0 (10.8)	892.6	(4.9)
14	Riverine, seasonally saturated, forested	68.0 (9.7)	276.9 (39.5)	31.4 (4.5)	168.0 (24.0)	149.2 (21.3)	7.6 (1.1)	701.2	(3.9)
15	Riverine, seasonally saturated, non-forested	202.7 (10.0)	1109.1 (54.6)	165.6 (8.2)	270.5 (13.3)	233.1 (11.5)	50.4 (2.5)	2031.3	(11.2)
16	Palustrine, regularly flooded, forested	1.4 (2.0)	11.6 (15.9)	5.9 (8.1)	48.9 (67.5)	4.3 (5.9)	0.4 (0.6)	72.5	(0.4)
17	Palustrine, regularly flooded, non-forested	3.3 (2.8)	26.1 (22.3)	6.3 (5.4)	74.7 (63.6)	5.8 (5.0)	1.3 (1.1)	117.5	(0.6)
18	Palustrine, seasonally saturated, forested	7.3 (5.2)	28.1 (20.3)	11.1 (8.0)	82.0 (59.2)	9.2 (6.6)	0.9 (0.7)	138.5	(0.8)
19	Palustrine, seasonally saturated, non-forested	32.6 (10.8)	102.2 (33.9)	28.4 (9.4)	109.1 (36.2)	21.2 (7.0)	8.1 (2.7)	301.7	(1.7)
20	Ephemeral, forested	4.9 (13.3)	16.0 (42.8)	1.5 (4.0)	7.8 (21.0)	6.1 (16.5)	0.9 (2.4)	37.3	(0.2)
21	Ephemeral, non-forested	12.0 (5.5)	96.9 (44.2)	10.4 (4.7)	32.4 (14.8)	32.8 (15)	34.6 (15.8)	219.1	(1.2)
22	Arctic/boreal peatland, forested	0.0 (0.0)	737.2 (52.3)	21.3 (1.5)	651.9 (46.2)	0.0 (0.0)	0.0 (0.0)	1410.4	(7.8)
23	Arctic/boreal peatland, non-forested	0.0 (0.0)	858.7 (66.8)	18.7 (1.5)	408.8 (31.8)	0.0 (0.0)	0.0 (0.0)	1286.1	(7.1)
24	Temperate peatland, forested	1.4 (0.3)	143.3 (33.2)	97.2 (22.5)	162.3 (37.6)	15.7 (3.6)	11.7 (2.7)	431.7	(2.4)
25	Temperate peatland, non-forested	0.5 (0.2)	94.3 (40.5)	80.3 (34.5)	39.7 (17.1)	15.3 (6.6)	2.6 (1.1)	232.8	(1.3)
26	Tropical/subtropical peatland, forested	129.0 (16.1)	294.4 (36.6)	0.0 (0.0)	21.6 (2.7)	313.9 (39.1)	44.6 (5.6)	803.5	(4.4)
27	Tropical/subtropical peatland, non-forested	7.3 (7.0)	47.2 (45.7)	0.0 (0.0)	10.9 (10.5)	33.4 (32.3)	4.6 (4.5)	103.3	(0.6)
28	Mangrove	29.3 (19.4)	59.8 (39.7)	0.4 (0.3)	23.8 (15.8)	20.5 (13.6)	16.9 (11.2)	150.8	(0.8)
29	Saltmarsh	2.3 (4.0)	11.6 (19.6)	6.0 (10.1)	32.1 (54.2)	4.7 (7.9)	2.5 (4.2)	59.2	(0.3)
30	Large river delta	19.6 (7.0)	148.7 (53.3)	12.8 (4.6)	36.8 (13.2)	60.3 (21.6)	0.6 (0.2)	278.7	(1.5)
31	Other coastal wetland	29.2 (7.9)	133.5 (36.3)	33.1 (9.0)	98.9 (26.9)	35.9 (9.8)	37.1 (10.1)	367.8	(2.0)
32	Salt pan, saline/brackish wetland	109.9 (24.5)	98.1 (21.9)	92.4 (20.6)	18.5 (4.1)	57.1 (12.7)	71.9 (16.0)	447.9	(2.5)
33	Paddy rice	53.7 (4.4)	1034.8 (85.7)	22.0 (1.8)	33.6 (2.8)	45.7 (3.8)	17.4 (1.4)	1207.1	(6.6)
<b>Total wetlands [10<sup>6</sup> km<sup>2</sup>] (% among all wetlands)</b>		<b>1.60 (8.8)</b>	<b>7.97 (43.8)</b>	<b>1.11 (6.1)</b>	<b>4.86 (26.7)</b>	<b>2.10 (11.6)</b>	<b>0.55 (3.0)</b>	<b>18.19</b>	<b>(100)</b>
<b>Total land [10<sup>6</sup> km<sup>2</sup>] (% wetland-to-land ratio)</b>		<b>29.9 (5.3)</b>	<b>42.7 (18.7)</b>	<b>12.0 (9.3)</b>	<b>24.4 (19.9)</b>	<b>17.8 (11.8)</b>	<b>8.5 (6.5)</b>	<b>135.3</b>	<b>(13.4)</b>



545

**Figure 4: Total wetland extent as estimated by Global Lakes and Wetlands Database (GLWD) v2. Values show percent coverage for all wetland classes combined per 500 m grid cell. Total wetland extent in each cell is bounded to 1-100%; cells with 0% wetland extent are classified as dryland.**

#### 550 4.2 Wetland class distribution

Grouping specific classes into broad categories reveals global trends of wetland distribution. Unsurprisingly, marine/coastal wetland classes cover only 5% of the total extent, while the majority of 95% of wetlands are inland. Waterbody classes occupy 23% of the total wetland extent while other wetland classes, including emergent and bare wetlands, occupy 77%. Freshwater marshes (i.e., non-forested) and freshwater swamps (i.e., forested) (combined classes 8-21) compose 39% of all wetlands, with two-thirds being marshes (64%) and one-third swamps (36%). Within these marsh and swamp areas, the vast majority (68%) is seasonally flooded or saturated, highlighting the strong intra-annual variability in extent of these wetlands, while 16% are regularly flooded, 4% are ephemeral, and 13% are lacustrine wetlands with no specified periodicity (total not summing to 100% due to rounding). When these marsh and swamp wetlands are grouped by flooding source, riverine wetlands account for the largest share (75%), followed by lacustrine (13%), palustrine (9%), and ephemeral (4%) wetlands.

560

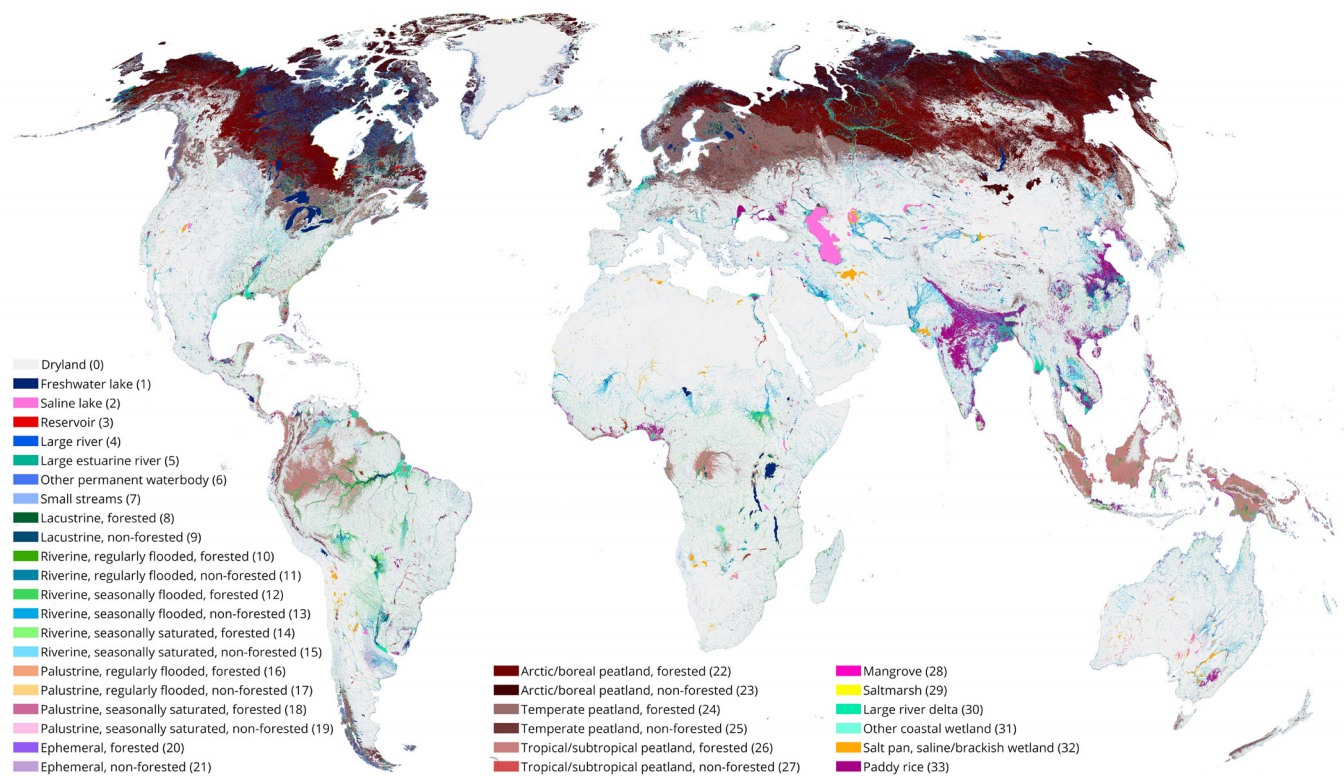


**Figure 5: Dominant wetland class for each 500 m grid cell of the Global Lakes and Wetlands Database (GLWD) v2. Total wetland extent in each cell is bounded to 1-100%; cells with 0% wetland extent are classified as dryland. Legend classes include numerical class values in parentheses.**

565

A more granular inspection of individual classes highlights the predominance of specific wetland types. Among the 33 classes (Table 3 and Figure 5), five classes exceed 1 million km<sup>2</sup> globally: freshwater lakes (2.05 million km<sup>2</sup>, of which 60% are in North and Central America); riverine, seasonally saturated, non-forested wetlands (2.03 million km<sup>2</sup>); forested arctic/boreal peatlands (1.41 million km<sup>2</sup>); non-forested arctic/boreal peatlands (1.29 million km<sup>2</sup>); and paddy rice (1.21 million km<sup>2</sup>). All peatlands combined (arctic/boreal, temperate, and tropical/subtropical, both forested and non-forested) cover a total of 4.27 million km<sup>2</sup>, representing nearly a quarter (23%) of the total wetland extent on Earth (Table 3 and Figure 6). They emerge as the dominant wetland type across almost all northern latitudes above 50° N as well as parts of the tropics; however, as the organic soils of peatlands are difficult to map with remote sensing methods, the coarser resolution of the input source data used in GLWD v2 creates local uncertainties. Paddy rice (6.6% of total global wetland extent) occurs predominantly throughout southern and eastern Asia including India, northeast China, Vietnam, Thailand, Bangladesh, Sri Lanka, Myanmar, and, to a lesser extent, other regions such as the Nigerian coast and within the Mississippi floodplains (Figure 5). Various other waterbody and wetland classes are regionally dominant, including freshwater lakes in North

575



America and northern Eurasia; riverine wetlands in South America, Sub-Saharan Africa, and Asia; saline lakes in Central Asia; and ephemeral wetlands in Australia. Small streams occur as small percentages all around the world and dominate in locations where no other wetland type occurs; but they are not easily discernable on the global map (Figure 5) among other more prominent wetland classes.

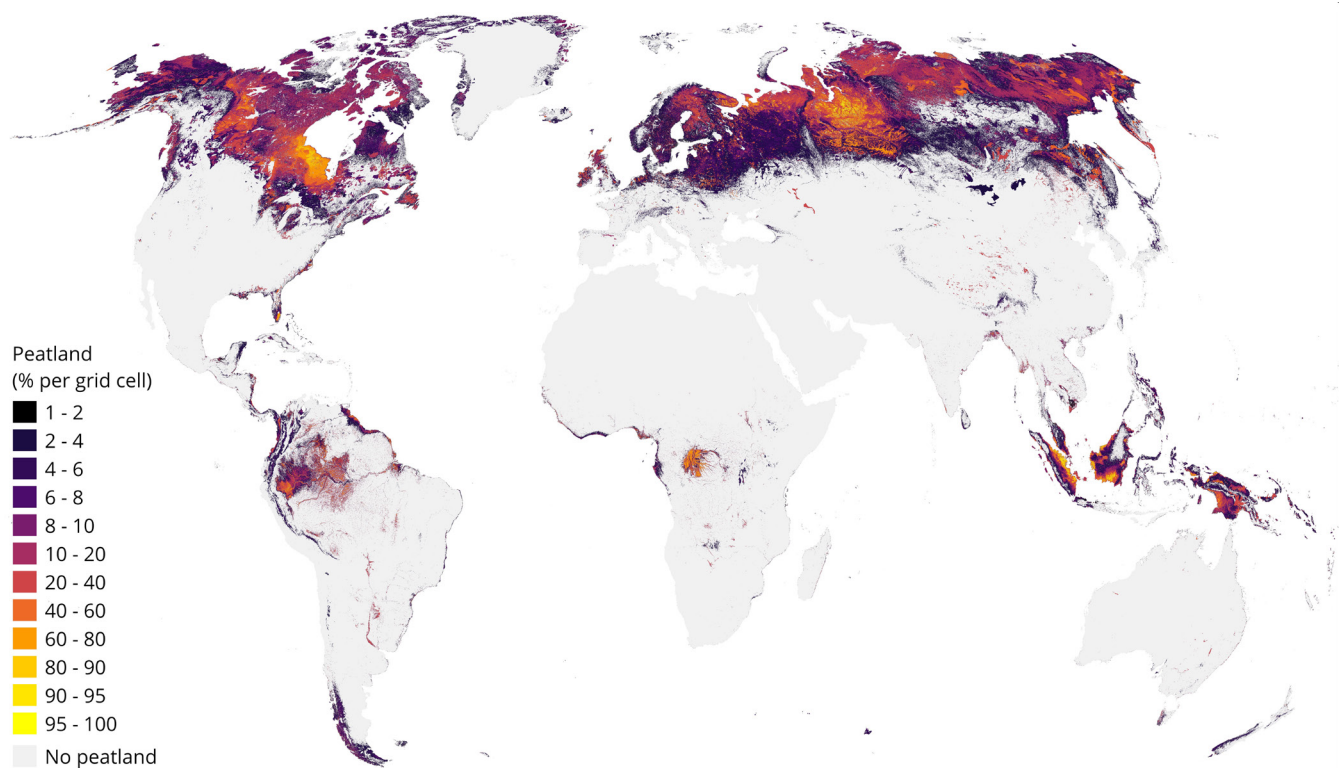


**Figure 6: Total peatland extent as estimated by the Global Lakes and Wetlands Database (GLWD) v2 for all 6 peatland classes combined (arctic/boreal, temperate, and tropical/subtropical; forested and non-forested). Values show percent coverage per 500 m grid cell. Total peatland extent in each cell is bounded to 1-100%; cells with 0% peatland extent are classified as no peatland.**

### 4.3 Comparison to independent data

The lack of systematic field data on wetland presence and type across the world precludes a direct validation of our broad-scale wetland maps. In lieu of ground-truthing using in situ samples, we compare the output of GLWD v2 against independent wetland extents reported in the literature, and we also situate our estimates relative to previous large-scale wetland maps and data compilations. However, differences in wetland definitions and the intrinsic temporal (both inter- and





intra-annual) variability of wetland extents can lead to vast discrepancies and preclude any one-to-one comparison. For  
595 example, a recent global wetland study produced synthetic sample points from compiled data sources (Zhang et al., 2023;  
2024), but the condensed eight wetland classes do not align with our approach or outputs. Nonetheless, we compare area  
estimates of GLWD v2 to those derived from several remote sensing analyses, compilations of national and regional surveys,  
model simulations, and statistical extrapolations. Table 4 provides an overview of the ranges of available global, regional,  
national, or large individual wetland extent estimates for various wetland types, including their sources.

#### 600 4.3.1 Total area comparisons

The global wetland extent of GLWD v2 (18.2 million km<sup>2</sup>) lies within the wide range of 2.0 to 30.5 million km<sup>2</sup> from  
literature (Table 4). In a review of global wetland datasets, Hu et al. (2017a) found that estimates from compilation datasets  
range between 2.8 and 12.7 million km<sup>2</sup> and estimates from remote-sensing approaches range between 2.1 and 17.3 million  
km<sup>2</sup>. GLWD v2 thus matches the high end of the remote sensing-based estimates. The much larger global wetland extent  
605 estimates of 27.5 and 30.5 million km<sup>2</sup> produced by Tootchi et al. (2019) and Lane et al. (2023), respectively, are partly  
explained by the inclusion of model-simulated wetlands that are determined by shallow groundwater occurrences.

The Amazon River Basin is a well-studied wetland hotspot and a frequently used benchmark for new wetland maps. The  
total wetland extent of GLWD v2 for the entire Amazon Basin is 834,300 km<sup>2</sup>, of which 444,400 km<sup>2</sup> are over lowland  
floodplains. Fleischmann et al. (2022) compared 29 inundation datasets over lowland regions (elevation <500 m) and  
610 estimated the upper bounds of the seasonal minimum and maximum extents as 284,200 km<sup>2</sup> and 872,700 km<sup>2</sup>, respectively.  
That the area of GLWD v2 falls within the range of these independent estimates demonstrates the ability of GLWD v2 to  
reasonably capture forested and seasonally inundated wetlands in the tropics, some of the most challenging wetland types to  
detect. The largest spatial discrepancies in this basin occur for interfluvial (or palustrine) wetlands characterized by  
shallower and more variable rainfall-driven flooding patterns than the more predictable riparian floodplains. To improve the  
615 identification of interfluvial wetland ecosystems, more refined efforts may be needed to include additional, small-scale  
parameters such as landform (or geomorphic setting) and vegetation (see also section 5.2).

Independent estimates of other large wetland extents across the world, including the Pantanal in South America; the Niger  
Inland Delta, Sudd Swamps, and Okavango Delta in Africa; and the Mesopotamian Marshes in the Middle East also confirm  
the overall reliable wetland coverage of GLWD v2, consistently near or within the literature estimates that are often wide-  
620 ranging (Table 4). One exception to this is the GLWD v2 estimate of 3.4 million km<sup>2</sup> of wetlands in Canada (34% of land  
area), more than double the national estimate of 1.3 million km<sup>2</sup> (13% of land area; Environment and Climate Change  
Canada, 2016). This discrepancy is explained by the maximalist perspective of GLWD v2 contrasting with the more  
restricted national definition. Moreover, the lower national estimate is exceeded by independent peatland and lake area  
estimates alone (Table 4), demonstrating the discrepancies originating from conflicting definitions and goals. This example  
625 underlines the value of GLWD v2 in providing a transparent and spatially explicit baseline of composite wetland extents  
using fractional cell coverages.



**Table 4: Comparisons of global and regional wetland extents.**

Wetland type [GLWD v2 class(es)]	Region	Extent [10 <sup>3</sup> km <sup>2</sup> ]		References (note that many references report on multiple wetland types and regions, thus only selected key references are listed here; multiple references for individual classes are sorted, where possible, from low to high estimates)
		GLWD v2	Other sources	
All types [1-33]	Global	18,187	2,000 – 30,500	Aselmann & Crutzen, 1989; Finlayson & Davidson, 1999; Fluet-Chouinard et al., 2015; Hu et al., 2017a, 2017b; Lane et al., 2023; Lehner & Döll, 2004; Lieth, 1975; Matthews & Fung, 1987; Melton et al., 2013; Mitsch & Gosselink, 2015; Prigent et al., 2007; Spiers, 2001; Tiner, 2009, 2015
	Canada	3,399	2,090 <sup>a</sup>	Tarnocai et al., 2011; Messenger et al., 2016
	Amazon Basin	444.4 - 834.3 <sup>b</sup>	25.0 – 872.7	Fleischmann et al., 2022
	Pantanal	106.4	138 – 160	Alho, 2005; Bergier & Assine, 2016; Mitsch & Gosselink, 2015
	Congo Cuvette Centrale	141.3	132 – 360 <sup>c</sup>	Dargie et al., 2017; Campbell, 2005; Bwangoy et al., 2010
	Sudd Swamps	64.9	30 – 57 – 130 <sup>d</sup>	Sutcliffe & Parks, 1999; Mohamed et al., 2004; Ramsar, 2006; Mulatu et al., 2022
	Niger Inland Delta	45.7	15 – 47	Gourcy et al., 2000; Ramsar, 2004; Sutcliffe & Parks, 1989
	Okavango Delta	7.4	2.5 – 16	McCarthy et al., 2003
	Mesopotamian Marshes	26.7	5.4 – 20 <sup>e</sup>	Ramsar, 2012, 2015a, 2015b; Al-Handal & Hu, 2015; Richardson & Hussain, 2006
Freshwater & saline lakes [1, 2]	Global	2,715	2,000 – 4,760 <sup>f</sup>	Mulholland & Elwood, 1982; Downing et al., 2006; Messenger et al., 2016; Pi et al., 2022; Verpoorter et al., 2014
Reservoirs [3]	Global	315.7	251.0 – 492.1	Lehner & Döll, 2004; Downing et al., 2006; Lehner et al., 2011; Wang et al., 2021
Rivers [4, 5, 7]	Global	589.3	404.0 <sup>g</sup> – 662.0	Allen & Pavelsky, 2018; Raymond et al., 2013; Downing et al., 2012
	USA	41.0	30.4	Dahl, 2011
Forest swamp [8, 10, 12, 14, 16, 18, 20]	Global	880.0 <sup>h</sup> – 2,562	1,087 – 1,370	Matthews & Fung, 1987; Gumbricht et al., 2017
	USA	30.9 <sup>h</sup> – 166.5	208.9	Dahl, 2011
Freshwater marsh [9, 11, 13, 15, 17, 19, 21]	Global	1,173 <sup>h</sup> – 4,618	274.0 – 2,787	Aselmann & Crutzen, 1989; Gumbricht et al., 2017
	China	97.7 <sup>h</sup> – 590.8	217.3 <sup>i</sup>	Sun et al., 2015
	USA	40.9 <sup>h</sup> – 281.2	185.9 <sup>j</sup>	Dahl, 2011
Peatland [22, 23, 24, 25, 26, 27]	Global	4,268	3,700 <sup>k</sup> – 4,232	Hugelius et al., 2020; Joosten, 2009; Dugan, 1993; Xu et al., 2018
	Canada	1,068	1,136	Tarnocai et al. 2011
	Finland	48.5	90.0	Tanneberger et al., 2017
	Germany	10.2	12.8	Tanneberger et al., 2017
Tropical/subtropical peatland [26, 27]	Global	906.9	441.0 – 1,700	Page et al., 2011; Gumbricht et al., 2017
	Brazil	170.2	25.0 – 312.3	Page et al., 2011; Gumbricht et al., 2017
	DR Congo	67.3	2.8 – 115.6	Page et al., 2011; Gumbricht et al., 2017
	Indonesia	260.6	207.0 – 265.5	Page et al., 2011; Gumbricht et al., 2017
Mangrove [28]	Global	150.8	137.6 – 166.0	Bunting et al., 2018; Giri et al., 2011; Spalding et al. 2010; Sanderman et al., 2018
	Indonesia	30.3	29.5	Bunting et al., 2022
	USA	2.4	2.8	Dahl, 2011
Saltmarsh [29]	Global	59.2	22.0 <sup>l</sup> – 400.0 <sup>m</sup>	Chmura et al., 2003; Mcowen et al., 2017; Duarte et al., 2005; Woodwell et al., 1973
	USA	19.9	15.6 – 18.5	Dahl, 2011; Worthington et al., 2024
	Canada	8.7	3.6	Rabinowitz & Andrews, 2022
Large river delta [30]	Global	278.7	305.9 – 710.2	Syvitski et al., 2009; Ericson et al., 2006; Tessler et al., 2015; Edmonds et al., 2020
	Amazon	32.9 – 72.1 <sup>n</sup>	160.0 – 467.0	Edmonds et al., 2020
Coastal wetland [28, 29, 30, 31]	Global	856.4	160.0 – 540.0	Najjar et al., 2018; Nicholls et al., 1999; Pendleton et al., 2012
	Global	1,207	1,138 – 1,663	Yu et al., 2020; Rosegrant et al., 2002; Portmann et al., 2010; FAOSTAT, 2024
Paddy rice [33]	China	239.6	174.7 – 289.5 <sup>p</sup>	Yu et al., 2020; National Bureau of Statistics of the People's Republic of China, 2023
	India	524.8	304.6 – 464.0 <sup>p</sup>	Yu et al., 2020; Government of India, 2023
	Nigeria	26.8	18.0 – 45.8 <sup>p</sup>	Federal Republic of Nigeria, 2009; FAOSTAT, 2024

<sup>a</sup> Sum of total peatland (Tarnocai et al., 2011) and lake extent (Messenger et al., 2016)

<sup>b</sup> Low estimate is for lowland floodplains, high estimate is for entire Amazon Basin

<sup>c</sup> Low estimate is for peatland only, high estimate includes all (seasonal) wetlands

<sup>d</sup> Low and middle estimates are for permanent and seasonal swamps, high estimate is for extreme flooding (Mulatu et al., 2022)

<sup>e</sup> High estimate is for pre-desiccation marshland extent (i.e., before 1991); low estimate is for post-desiccation (i.e., start of restoration efforts after 2003)

<sup>f</sup> Including extrapolations to lakes ≥ 1 ha

<sup>g</sup> Estimate for rivers wider than 90 m

630

635





<sup>h</sup> Counting only riverine classes that are regularly or seasonally flooded (rather than saturated, or undefined in the case of lacustrine and ephemeral classes)

<sup>i</sup> Estimate for marshes and swamps

<sup>j</sup> Estimate for freshwater marshes/wet meadows and shrub wetlands

<sup>k</sup> Estimate of northern peatlands only (>23°N latitude)

640 <sup>l</sup> From Chmura et al. (2003), based on inventories from Canada, Europe, US, and South Africa

<sup>m</sup> From Woodwell et al. (1973), extrapolated only from data from the US and not expecting an accuracy within +/-50%

<sup>n</sup> Low estimate is for class 30 (large river delta) only, high estimate is for all wetland classes within delta region

<sup>o</sup> Sum of maximum reported extents of mangrove, saltmarsh, and river delta in previous rows

<sup>p</sup> High estimate for harvested area, meaning that land cropped for rice multiple times in a year is counted multiple times

645

### 4.3.2 Per-class comparisons

We consider comparisons of individual classes with independent estimates from the literature to be more meaningful in cases where multiple literature estimates converge around a tighter range of values. Therefore, we evaluated GLWD v2 classes by groups tiered by the difference between the maximum and minimum areas found in literature: strong agreement (<2-fold  
650 discrepancy), moderate agreement (2-3-fold) and poor agreement (>3-fold).

GLWD v2 classes with strong agreement in literature include reservoirs, rivers, forest swamps, peatlands, mangroves, and paddy rice. Of those classes, all but forest swamps and paddy rice show good agreement between GLWD v2 and global or national independent estimates, with GLWD v2 often falling at the higher end of the reported range. For paddy rice extents, the global area of GLWD v2 agrees well with the global *physical* area but is closer to *harvested* area in some countries  
655 (accounting for multiple cropping cycles), suggesting either a regional overestimate by GLWD v2 or a potential interannual change in physical area or the type of cropping (see Table 4 for country-level examples). In contrast, GLWD v2 estimates for forest swamps are substantially higher than literature because GLWD v2 broadly defines forest swamps as any inundated area (not otherwise claimed by a different wetland class) with >10% tree coverage whereas other definitions of forest swamps also consider more demanding criteria such as soil moisture and hydrophytic vegetation.

660 Wetland types with moderate literature agreement include lakes and river deltas. In the case of lakes, discrepancies with literature arise depending on the smallest lake size accounted for, i.e., whether estimates were extrapolated to smaller or even undetectable ponds. GLWD v2 explicitly classifies lakes with a surface area of at least 10 ha, which falls within the range found in literature, and many smaller lakes are expected to be included within the ‘other permanent waterbody’ class. For large river deltas, disagreements in literature estimates about global extents are largely due to the different approaches in  
665 delineating the boundaries of deltas from satellite imagery or topographical data, often leading to only coarse outlines of the delta region as a whole. The GLWD v2 estimate for large river deltas is lower than independent estimates in part because we prioritized explicit wetland classes, such as rivers, lakes, and paddy rice, over the generic ‘large river delta’ class in cases of overlap (e.g., Amazon Delta in Table 4).

670 Finally, wetland types with poor literature agreement include freshwater marshes, tropical/subtropical peatlands, and saltmarshes. Diverging estimates both within literature and to GLWD v2 are due to multiple issues, including differences in wetland definitions, small wetland occurrences relative to mapping resolutions, difficulties in detection through remote sensors, and sparse and incomplete reporting. Recent methodological improvements have led to larger estimated extents of



675 some classes over time. For example, benefitting from improved remote sensing and field data, tropical peatland complexes  
in Africa and South America have been mapped to exceed earlier estimates, indicating that previous studies have  
underestimated their extent. As GLWD v2 incorporates some of the most recent maps of global peatland and saltmarsh  
680 extents, it captures a similar total area as referenced in these sources. This also confirms that the multi-step merging process  
did not cause substantial distortion of original data. Saltmarshes may still be underestimated by GLWD v2 globally, but data  
quality and completeness varies regionally as shown by the larger saltmarsh areas for the US and Canada in GLWD v2  
compared to literature estimates. The area of freshwater marshes estimated by GLWD v2 is substantially higher than the  
680 literature range because GLWD v2 uses freshwater marshes as a catch-all class for all inundated wetland—not otherwise  
classified—with sparse vegetation cover (<10% forest). This goes far beyond the definitions from literature, which tend to  
rely on narrower interpretations of vegetation types and soil moisture conditions to identify freshwater marshes (often in  
ways applicable only to a specific region).

## 5 Discussion

685 GLWD v2 provides a comprehensive representation of the world's wetland ecosystems by harmonizing state-of-the-art data  
sources at grid cell resolutions ranging from ~10 m to 1 km into a target resolution of 500 m. By drawing on global or near-  
global inputs, 33 individual wetland classes were mapped consistently across the world, avoiding regional discrepancies that  
can emerge from a patchwork of regional or national data sources. The 33 resulting classes of GLWD v2 improve upon  
previously available maps, including GLWD v1, thereby helping to close the gap between field inventory typologies and  
690 globally applicable classifications (Davidson et al., 2018).

The reliability of different classes depends on their respective data sources and associated data manipulation and  
interpretation. The recent growth of optical imagery archives has resulted in high-quality maps of inland surface water,  
including lakes and rivers, that were directly incorporated into GLWD v2 without substantial alteration. Certain explicit  
wetland types, such as mangroves and saltmarshes, were available as detailed maps requiring only limited modifications,  
695 whereas other classes, such as peatlands or paddy rice, were derived from coarser historical maps or synthesized from  
multiple input maps. Wetland areas defined broadly as seasonal inundation or saturation, including lacustrine, riverine, and  
palustrine wetlands, were more challenging to delineate directly from satellite imagery. These inundated/saturated wetlands  
were mapped from coarse-resolution multi-sensor estimates spanning over two decades that were downscaled using  
topography to represent average inundation frequencies which were combined with ancillary data to produce wetland  
700 classes.

### 5.1 All-inclusive wetland definition and applied criteria

The compilation of GLWD v2 was carried out with the objective of including all wetlands at their maximum extent rather  
than enforcing strict wetland type definitions. As a result, each wetland type is determined by a distinct set of criteria,



705 resulting from the approaches and constraints of the original data sources, rather than a single harmonized definition. Different wetland classes were specified by a combination of spatial, temporal, and ancillary characteristics, and can be grouped into three broad categories: waterbodies, other inland wetlands, and other coastal wetlands (Figure 2). Aside from the exceptions described in the Methods, the following general class characterizations can be distilled from our data fusion procedures and merger rules:

- 710 • Waterbodies comprise open water surfaces wider than 30 m for rivers and larger than 10 ha for lakes. Areas of small streams were predicted statistically for those exceeding 100 L/s in average flow or 10 km<sup>2</sup> in catchment size. Waterbodies generally have persistent presence of open water surfaces; however, specific waterbody types may not be fully inundated at all times; for example, reservoir polygons may delineate surfaces at high water levels, rivers may encompass multiple shifting channels, and a substantial number of small streams will experience intermittent flow. Other permanent waterbodies include, but are not differentiated for, additional parts of rivers, small lakes, ponds, and artificial water surfaces such as canals, as long as they exceed 30 m in width which reflects the detection limit of the used optical imagery.
- 715 • Other inland wetlands represent either periodically inundated or surface saturated areas of various frequencies, with or without forest cover, or represent organic peatland soils, rice paddies, or salt pans.
- 720 • Other coastal wetlands are defined by either a particular vegetation cover or are collectively defined as wetlands located less than 10 m above sea level and connected to the coastline, as these criteria were used across several of the data sources or were introduced during the data fusion process.

The broad wetland definition of GLWD v2 allows it to encompass most national definitions, except for specific wetland types that cannot be reliably mapped globally (e.g., explicit identification of aquaculture ponds, or presence of subterranean or geothermal wetlands). Setting aside missing classes, GLWD v2 may still underrepresent wetland extents due to the detection size and revisit period of observation systems, but not due to restrictions derived from definitions. With its broad wetland definition, GLWD v2 aims to address the widely shared concern that published global wetland extent estimates from either national inventories or remote sensing technology may still underestimate the true global wetland extent (Davidson et al., 2018).

## 5.2 Classification design and comparison to existing classification systems

730 The multiple factors used to categorize wetland types—including hydrology, inundation, soils, vegetation, landscape position, and connectivity—allow GLWD v2 to represent a wide variety of wetland conditions while filling the need for a generalized and manageable classification system. In particular, the inclusion of criteria beyond inundation, such as vegetation and soil conditions, more closely aligns GLWD v2 with field-based and national classifications and inventories (Gerbeaux et al., 2016; Ramsar Convention on Wetlands, 2002). In certain regions, GLWD v2 reaches a level of detail comparable to national and regional classification schemes.



740 GLWD v2 does not follow a strictly hierarchical classification approach with one specific criterion for subdivisions at each level. Such an approach would yield a much larger number of subclasses. Instead, our grouping of classes into a simplified, systematic but versatile classification system (Figure 2) allows users to combine classes in various ways for applications where fewer and/or broader classes are more useful. For instance, regrouping of classes can occur along various axes, including open water vs. vegetated, inundated vs. saturated, forested vs. non-forested, connected to waterbodies vs. isolated, or mineral vs. organic soils.

745 The design of GLWD v2 classes stemmed from two primary methodological procedures: First, we harmonized existing maps of explicit wetland types. In this process, we selected one representative dataset per class (e.g., one river dataset) wherever possible to reduce the issue of double-counting or temporal mismatches for overlapping water features. Second, once all pre-defined classes were harmonized, we classified the extent of indiscriminate inundation by attaching hierarchical labels. This classification of indiscriminate inundation incorporates ideas from several classification schemes. We elected to combine components of the “*landscape position, landform, water flow path and waterbody type (LLWW) descriptors*” (Tiner, 2014) along with simple biotic discriminants (forested vs. non-forested). The classification in GLWD v2 diverges from proposed hydro-geomorphic wetland classification schemes (e.g., Brinson, 1993; Semeniuk & Semeniuk, 1995) by not including landform (slope, channel, depression, etc.) among its criteria, not least due to the lack of high-precision input data to determine small-scale geomorphic features. Instead, GLWD v2 uses inundation and saturation frequency as well as spatial connectivity between wetland ecosystems via contiguous surface water extents as a proxy for hydrological, biogeochemical, and ecological connectivity. This is also why inundation extents and frequencies from GIEMS-D3 and the CaMa-Flood hydrological model were chosen as inputs over purely topographical definitions of floodplains such as those produced by Tootchi et al. (2019) and Lane et al. (2023).

750 Although GLWD v2 presents a novel classification scheme, its typology shares basic similarities with some of the most common classification systems, including those of the IUCN’s Ecosystem Functional Groups (EFGs) (Keith et al., 2022), the US National Wetland Inventory (Cowardin et al., 1979), and the Ramsar Convention on Wetlands (Table 5). Although classes rarely have one-to-one equivalencies, several comparable groupings emerge. GLWD v2 is less detailed than IUCN’s EFGs for waterbodies but offers more levels of separation for other freshwater wetlands (28 EFGs qualify as wetlands). To increase concordance with the IUCN system and facilitate potential crosswalks of classifications, the simplified representation of rivers and lakes in GLWD v2 could be further expanded by employing ancillary datasets for river types (e.g., the Global River Classification (GloRiC); Ouellet Dallaire et al., 2019) and lake characteristics (e.g., LakeATLAS; Lehner et al., 2022). An analogous division into bioclimatic regions as proposed in the IUCN typology (e.g., tropical, temperate, alpine, etc.) could also be added to GLWD v2.

765 GLWD v2 generally aligns well and shares nomenclature with the system and subsystem levels of the US National Wetland Inventory (hereafter NWI; Cowardin et al., 1979; Cowardin & Golet, 1995), a classification of wetlands and deep-water habitats used by the US Fish & Wildlife Service. Comparing higher levels of classification hierarchy, GLWD v2 applies its landscape connectivity labels (lacustrine, riverine, or coastal) far more broadly than NWI does, as GLWD v2 is inspired by



770 the LLWW approach. At the lower levels of classification, GLWD v2 follows a vegetation dichotomy similar to the more  
 numerous ‘modifiers’ used by NWI (e.g., vegetation, soil, sediment). Finally, the Ramsar Convention’s classification, which  
 was gradually expanded over time to accommodate the diversity of the world’s wetlands and later simplified in the Global  
 Wetland Outlook (Davidson & Finlayson, 2018), covers a similarly large breadth of wetlands as GLWD v2. However, the  
 ambiguity and overlap between some of the Ramsar class definitions (Semeniuk & Semeniuk, 1997; Finlayson, 2016)  
 775 present relatively few direct equivalencies with GLWD v2 wetland classes.

**Table 5: Class equivalency between GLWD v2 and common global wetland typologies: the wetland and deep-water  
 classification of the US National Wetland Inventory (NWI) (Cowardin et al., 1979), the classification of the Ramsar  
 Convention on Wetlands, the simplified Ramsar types of the Global Wetland Outlook (GWO) (Davidson &  
 780 Finlayson, 2018) and the IUCN global Ecosystem Functional Groups (EFGs) (Keith et al., 2022). Classes listed on the  
 same row signify partial equivalence, ranging from incomplete overlap to complete nestedness. Additional class  
 overlaps are possible depending on application and we recommend case-by-case re-evaluation of this crosswalk. Some  
 classes from Ramsar, GWO and NWI are not listed on the table because of the absence of an equivalent class in  
 GLWD v2. Class names were modified for brevity.**

785

GLWD v2 Class ID and Name	NWI Classification (system, subsystem, water regime modifier)	Ramsar Convention on Wetland’s type classification system	Global Wetland Outlook (classes/subclasses)	IUCN Ecosystem Functional Groups (EFGs)
1. Freshwater lake	Lacustrine, Limnetic	K- Coastal freshwater lagoons O- Permanent freshwater lakes P- Seasonal/intermittent freshwater lakes	Natural lakes ≥10ha	F2.1 – Large permanent freshwater lakes F2.2 – Small permanent freshwater lakes F2.3 – Seasonal freshwater lakes F2.4 – Freeze-thaw freshwater lakes
2. Saline lake	Lacustrine, Limnetic	Q- Permanent saline/brackish lakes	Natural lakes ≥10ha	F2.6 – Permanent salt and soda lakes F2.7 – Ephemeral salt lakes
3. Reservoir	Lacustrine, Limnetic	6- Water storage areas	Reservoirs	F3.1 – Large reservoirs
4. Large river	Riverine, Lower Perennial	M- Permanent rivers/streams/creeks	Rivers & streams	F1.2 – Permanent lowland rivers F1.3 – Freeze-thaw rivers and streams F1.5 – Seasonal lowland rivers F1.7 – Large lowland rivers
5. Large estuarine river	Riverine, Tidal	F- Estuarine waters	Rivers & streams	FM1.2 – Permanent open riverine estuaries and bays
6. Other permanent waterbody		8- Wastewater treatment areas 9- Canals and ditches	Lakes & pools <10 ha Small/farm ponds	F2.5 – Ephemeral freshwater lakes
7. Small streams	Riverine, Upper Perennial and Intermittent	N- Seasonal/intermittent rivers/streams	Rivers & streams	F1.1 – Permanent upland streams F1.4 – Seasonal upland streams F1.6 – Episodic arid rivers
8. Lacustrine, forested	Palustrine, Forested	W- Shrub-dominated wetlands Xf- Freshwater, tree-dominated wetlands Tp- Permanent freshwater marshes/pools	Forested wetlands	TF1.1 – Tropical flooded forests and peat forests TF1.2 – Subtropical/temperate forested wetlands
9. Lacustrine, non-forested	Lacustrine, Littoral Palustrine, Emergent	Ts- Seasonal/intermittent freshwater marshes/pools	Marshes & swamps	TF1.3 – Permanent marshes
10. Riverine, regularly flooded, forested	Palustrine, Forested	L- Permanent inland deltas W- Shrub-dominated wetlands Xf- Freshwater, tree-dominated wetlands	Forested wetlands	TF1.1 – Tropical flooded forests and peat forests TF1.2 – Subtropical/temperate forested wetlands
11. Riverine, regularly flooded, non-forested	Palustrine, Emergent	L- Permanent inland deltas Tp- Permanent freshwater marshes/pools	Marshes & swamps	TF1.3 – Permanent marshes
12. Riverine, seasonally flooded, forested	Palustrine, Forested	L- Permanent inland deltas W- Shrub-dominated wetlands Xf- Freshwater, tree-dominated wetlands	Forested wetlands	TF1.1 – Tropical flooded forests and peat forests TF1.2 – Subtropical/temperate forested wetlands
13. Riverine, seasonally flooded, non-forested	Palustrine, Emergent	Ts- Seasonal/intermittent freshwater marshes/pools	Marshes & swamps	TF1.4 – Seasonal floodplain marshes
14. Riverine, seasonally saturated, forested	Palustrine, Forested	W- Shrub-dominated wetlands Xf- Seasonal freshwater, tree-dominated	Forested wetlands	TF1.1 – Tropical flooded forests and peat forests TF1.2 – Subtropical/temperate forested wetlands



wetlands				
15. Riverine, seasonally saturated, non-forested	Palustrine, Emergent	Tp- Permanent freshwater marshes/pools Ts- Seasonal/intermittent freshwater marshes/pools	Marshes & swamps	TF1.4 – Seasonal floodplain marshes
16. Palustrine, regularly flooded, forested	Palustrine, Forested	W- Shrub-dominated wetlands	Forested wetlands	TF1.1 – Tropical flooded forests and peat forests TF1.2 – Subtropical/temperate forested wetlands
17. Palustrine, regularly flooded, non-forested	Palustrine, Emergent	Tp- Permanent freshwater marshes/pools	Marshes & swamps	TF1.3 – Permanent marshes
18. Palustrine, seasonally saturated, forested	Palustrine, Forested	W- Shrub-dominated wetlands Xf- Seasonal freshwater, tree-dominated wetlands	Forested wetlands	TF1.1 – Tropical flooded forests and peat forests TF1.2 – Subtropical/temperate forested wetlands
19. Palustrine, seasonally saturated, non-forested	Palustrine, Emergent	Ts- Seasonal/intermittent freshwater marshes/pools W- Shrub-dominated wetlands	Marshes & swamps	TF1.4 – Seasonal floodplain marshes
20. Ephemeral, forested	Palustrine, Forested	Xf- Seasonal freshwater, tree-dominated wetlands	Forested wetlands	
21. Ephemeral, non-forested	Palustrine, Emergent	W- Shrub-dominated wetlands Y- Freshwater springs/oases	Marshes & swamps	TF1.5 – Episodic arid floodplains
22. Arctic/boreal peatland, forested	Palustrine, Organic soil	Xp- Forested peatlands and peatswamp	Forested peatlands	TF1.6 – Boreal, temperate, and montane peat bogs
23. Arctic/boreal peatland/non-forested		U- Non-forested peatlands	Non-forested peatlands	TF1.6 – Boreal, temperate, montane peat bogs
24. Temperate peatland, forested	Palustrine, Organic soil	Xp- Forested peatlands and peatswamp	Forested peatlands	TF1.6 – Boreal, temperate, montane peat bogs
25. Temperate peatland, non-forested		U- Non-forested peatlands	Non-forested peatlands	TF1.6 – Boreal, temperate, montane peat bogs
26. Tropical/subtropical peatland, forested	Palustrine, Organic soil	Xp- Forested peatlands and peatswamp	Forested peatlands	TF1.1 – Tropical flooded forests and peat forests
27. Tropical/subtropical peatland, non-forested		U- Non-forested peatlands	Non-forested peatlands	TF1.1 – Tropical flooded forests and peat forests
28. Mangrove	Marine, Subtidal and Intertidal	H- Intertidal forested wetlands	Mangroves	MFT1.2 – Intertidal forests and shrublands
29. Saltmarsh	Estuarine, Intertidal	G- Intertidal marshes F- Estuarine waters	Saltmarshes	MFT1.3 – Coastal saltmarshes and reedbeds
30. Large river delta	Estuarine, Intertidal	H- Intertidal forested wetlands D- Rocky marine shores E- Sand, shingle, or pebble shores	Coastal deltas	MFT1.1 – Coastal river deltas
31. Other coastal	Estuarine, Intertidal	J- Coastal brackish/saline lagoons H- Intertidal forested wetlands	Unvegetated tidal flats Coastal lagoons Shallow subtidal system	FM1.2 – Permanent open riverine estuaries and bays
32. Salt pan, saline/brackish wetland	Lacustrine, Limnetic, Intermittently Flooded	R- Seasonal saline/brackish lakes and flats Sp- Permanent saline/brackish marshes/pools Ss- Seasonal saline/brackish marshes/pools	Salt pans, salinas	F2.7 – Ephemeral salt lakes
33. Paddy rice	Palustrine, Emergent Wetland, Artificially Flooded	3- Irrigated land, including rice fields	Rice paddy	F3.3 – Rice paddies

### 5.3 Limitations and uncertainties

As a composite mapping product, GLWD v2 inherits the uncertainties and shortcomings of its data sources. Given the large diversity of input datasets, we refrain from discussing the quality of each source and instead refer the reader to their original publications. Despite our efforts to avoid or reduce double-counting of wetland surfaces and minimize uncertainties stemming from the fusion of diverse data sources, we acknowledge that such uncertainties, distortions, and overestimations likely exist in GLWD v2, especially at local scales and in areas where multiple source datasets overlap. For example, temporal misalignment between water and wetland features are expected across data sources, such as due to migrating channels or shifting littoral edges. Spatial or temporal overestimations may be caused by the insufficient resolution of some source datasets (e.g., by interpreting small wetland patches to cover an entire cell) or the preferential use of wet periods when mapping wetland extents. Spatial mismatches are also expected between data sources used for arctic/boreal, temperate, and tropical/subtropical peatlands due to differences in their definition of soil organic content and horizon depth, as well as





the accuracy of their distribution. Nonetheless, our comparisons of GLWD v2 to other datasets (section 4.3) suggest that these uncertainties are neither systematic nor sufficiently large to deviate from most literature estimates. The process of synthesizing multiple data sources through masking, merging, and compositing is essential to produce a comprehensive and coherent map with spatially explicit distinctions between classes, especially given the many different types of wetlands on Earth. However, our harmonization of input sources does not improve upon their individual qualities, hence the original datasets at their native resolutions remain the best sources for specific wetland types.

To be applicable globally, the typology of GLWD v2 simplifies distinctions of certain wetland types while also emphasizing globally observable characteristics. For example, we excluded or used proxy measures for field-level indicators that are not directly observable from space, such as water table depth, hydrophytic vegetation, soil condition, microtopography, bathymetry, and salinity (Tiner, 2016; Gallant, 2015). Similarly, plant productivity and nutrient status of wetland ecosystems are used in some national classifications (e.g., ombrotrophic bog vs. minerotrophic fen in the Canadian classification) but are not applicable globally due to missing information at the necessary level of detail to achieve a reliable discrimination. Moreover, these local key characteristics are of secondary importance to the dominant drivers of wetland condition at the global scale that we used for GLWD v2 (hydrology, vegetation, soil type, and landscape position).

The implementation of landscape position and surface connectivity between waterbodies and other wetlands required some notable simplifications that have caused GLWD v2 to deviate from more detailed inventories. First, the separation of coastal wetlands is based on connectivity to the marine coast, which is only a proxy for water salinity or tidal hydrodynamics. Second, lacustrine or riverine wetland types were labeled based on surface water connectivity to nearby lakes or rivers, but we did not seek to further separate wetlands fed by groundwater (Tootchi et al., 2019) or local runoff and rainfall (Fan & Miguez-Macho, 2011). Third, palustrine wetland types were intended to represent geographically isolated wetlands, but some can remain connected with waterbodies through subsurface flow (Cohen et al., 2016). Finally, surface inundation and saturation as depicted in our source datasets ignores non-saturated wet soil conditions, which, if added, may have provided further paths of connectivity.

Rather than being a time-resolved product, GLWD v2 depicts contemporary conditions and limited aspects of inundation periodicity (seasonal, ephemeral, etc.) as a static map. As such, it represents a long-term baseline and should not be used to directly infer or monitor trends over time in global wetland distribution. The input sources are limited to data without explicit temporality, and in many cases there may be mismatches between sources due to different temporal snapshots or time-integrated summaries (e.g., flood frequencies). A time-resolved version of GLWD v2 at regular intervals would require both a narrower selection of data sources and more lenient assumptions about wetland classes to conform with data limitations. Furthermore, temporal representation presents new challenges, such as the high uncertainties of transitional wetland systems that fluctuate between saline, brackish and freshwater types as salinity levels change in response to flooding or drying cycles. Overall, interannual variation in seasonally flooded areas is likely the norm rather than the exception, as exemplified by the analyses of Amazon floodplains (Fleischmann et al., 2022).



#### 5.4 Future of mapping wetland ecosystems globally

For continuous monitoring of different wetland types to be achieved, high-resolution remote sensing paired with novel modeling approaches and/or machine learning techniques are needed (e.g., Gallant, 2015; Murray et al., 2022; Bunting et al. 2023). Ideally, such efforts should be supported by wide networks of water level loggers adequately capturing the variety of wetlands across the world. With new satellite missions such as SWOT and NISAR, GLWD v2 may act as a baseline layer and offer a globally applicable classification system onto which new data streams can be added to evaluate decadal-scale changes (Biancamaria et al., 2016). In the future, harmonization of GLWD v2 with time-series information derived from Landsat and/or Sentinel (rivers, lakes, and other permanent surface water) and additional sources such as multi-satellite inundation products could form the backbone of a temporally dynamic representation of wetland ecosystems.

Improvements in spaceborne hydrology observations represent a key component to develop an enhanced approach to detect, classify, and monitor wetlands globally. Dependable estimates of soil surface moisture, sub-canopy inundation, refined topographic data and detection of hydrophytic vegetation would allow for more detailed and reliable class distinctions. Furthermore, the GLWD v2 classification could be expanded by adding labels to waterbodies based on their surroundings, leading to new classes such as ‘peatland lakes’ or ‘floodplain lakes’. Finally, the exploration of a hydro-geomorphic classification could be ideal for functional assessments of wetland ecosystem types and the services they provide (Semeniuk & Semeniuk, 1995; 2011; Davis et al., 2013).

#### 6 Data availability

The GLWD v2.0 database, as presented in this manuscript, is available under a CC-BY 4.0 license at <https://www.hydrosheds.org/products/glwd> and a copy has been deposited at the figshare data repository at <https://figshare.com/s/e40017f69f41f80d50df> (Lehner et al., 2024). *[Note: the temporary figshare URL is for review purposes and will be replaced with a permanent figshare DOI link upon acceptance of the manuscript.]*

#### 7 Conclusions

GLWD v2 synthesizes the best available maps and Earth observation data from the last ~30 years into a coherent typology of the world’s wetland ecosystems. The resulting 33 wetland types substantially narrow the gap between field-level classification systems designed for local monitoring or management and globally applicable classifications informing large-scale conservation strategies, Earth system modeling, and international policy making. GLWD v2 provides global maps of dominant wetland classes and fractional cell coverage of each class at 500 m resolution to enable a new generation of research and applications. As a comprehensive static wetland map of contemporary wetlands generated from satellite and ancillary data, GLWD v2 is an important step in the transition of wetland monitoring from a compilation task to a continuous observation process.



If coupled with time-series information from novel remote sensing technologies, GLWD v2 can provide a foundation to transition towards a monitoring system capable of evaluating trends and variations of individual wetland types. Until that time, GLWD v2 provides an important baseline of wetland extent and classification that can facilitate the derivation of indicators for tracking progress toward the UN's Sustainable Development Goal 6.6 of protecting water-related ecosystems.

865 Given the importance of wetlands at the nexus of water, climate, and biodiversity, the dataset can also inform international policy frameworks such as the Convention on Biological Diversity (CBD), the Convention on Migratory Species (CMS), the Intergovernmental Science-Policy Platform on Biodiversity and Ecosystem Services (IPBES), the Ramsar Convention on Wetlands, and the United Nations Framework Convention on Climate Change (UNFCCC), among others.

### 8 Author contribution

870 Conceptualization: BL, EF, FA, PB, JGC, ND, CMF, TG, LH, GH, RBJ, PBM, SN, DO, JFP, BP, CP, DY, with support from all authors; Methodology: BL, MA, EF, BP, DY, with support from all authors; Data Contribution: BL, EF, FA, GHA, TG, GH, MCK, DO, TMP, JFP, CP, JW, TAW, DY; Data Curation: MA, BL; Software, Validation, Visualization: MA, EF, BL; Formal Analysis: BL, MA; Writing—Original Draft: MA, EF, FT, BL; Writing—Review and Editing: BL, with contributions and approval from all authors; Project Administration and Supervision: BL; Funding Acquisition: BL, MT.

### 875 9 Competing interests

The authors declare that they have no conflict of interest.

### 10 Acknowledgements

The development of the GLWD v2 database was initiated during a workshop on “Mapping the Global Extent and Dynamics of Freshwater Wetlands for CH<sub>4</sub> Emissions Modeling” in Washington, DC, in 2017, organized by Stanford University on behalf of the Global Carbon Project – Methane Budget. Financial support for the creation of the database was provided by 880 World Wildlife Fund, Washington, DC, and by The Nature Conservancy, Arlington, VA. The authors wish to express their gratitude to the many contributors beyond the list of co-authors, for their feedback and advice on the design of the database and/or in providing input data along the path of creating GLWD v2. Special thanks are due to Elaine Matthews for her inspiring efforts in advancing global wetland mapping, including her support on the design of this product, throughout her 885 career.



## References

- Aires, F., Miolane, L., Prigent, C., Pham, B., Fluet-Chouinard, E., Lehner, B., and Papa, F.: A Global Dynamic Long-Term Inundation Extent Dataset at High Spatial Resolution Derived through Downscaling of Satellite Observations, *J. Hydrometeorol.*, 18, 1305-1325, <https://doi.org/10.1175/jhm-d-16-0155.1>, 2017.
- 890 Al-Handal, A. and Hu, C. M.: MODIS Observations of Human-Induced Changes in the Mesopotamian Marshes in Iraq, *Wetlands*, 35, 31-40, <https://doi.org/10.1007/s13157-014-0590-6>, 2015.
- Alho, C. J. R.: The Pantanal, in: *The World's Largest Wetlands: Ecology and Conservation*, edited by: Fraser, L. H., and Keddy, P. A., Cambridge University Press, Cambridge, 203-271, <https://doi.org/10.1017/CBO9780511542091.008>, 2005.
- 895 Allen, G. H. and Pavelsky, T. M.: Global extent of rivers and streams, *Science*, 361, 585-587, <https://doi.org/10.1126/science.aat0636>, 2018.
- Allen, G. H., Pavelsky, T. M., Barefoot, E. A., Lamb, M. P., Butman, D., Tashie, A., and Gleason, C. J.: Similarity of stream width distributions across headwater systems, *Nat. Commun.*, 9, 610, <https://doi.org/10.1038/s41467-018-02991-w>, 2018.
- 900 Altenau, E. H., Pavelsky, T. M., Durand, M. T., Yang, X., Frasson, R. P. D., and Bendezu, L.: The Surface Water and Ocean Topography (SWOT) Mission River Database (SWORD): A Global River Network for Satellite Data Products, *Water Resour. Res.*, 57, e2021WR030054, <https://doi.org/10.1029/2021wr030054>, 2021.
- Aselmann, I. and Crutzen, P. J.: Global distribution of natural freshwater wetlands and rice paddies, their net primary productivity, seasonality and possible methane emissions, *J. Atmos. Chem.*, 8, 307-358, <https://doi.org/10.1007/BF00052709>, 1989.
- 905 Bergier, I. and Assine, M. L.: Dynamics of the Pantanal Wetland in South America, 1, *The Handbook of Environmental Chemistry*, Springer Cham, <https://doi.org/10.1007/978-3-319-18735-8>, 2016.
- Bernard, J., Fluet-Chouinard, E., Zhang, Z., Jimenez, C., and Prigent C.: Methane-centric global inundated extent from multi-sensor method (GIEMS-MC), in prep.
- 910 Biancamaria, S., Lettenmaier, D. P., and Pavelsky, T. M.: The SWOT Mission and Its Capabilities for Land Hydrology, *Surv. Geophys.*, 37, 307-337, <https://doi.org/10.1007/s10712-015-9346-y>, 2016.
- Brinson, M. M.: A hydrogeomorphic classification for wetlands, Technical Report WRP-DE-4, U.S. Army Engineer Waterways Experiment Station, Vicksburg, MS, 101 pp., <https://wetlands.el.erdc.dren.mil/pdfs/wrpde4.pdf>, 1993.
- Bunting, P., Hilarides, L., Rosenqvist, A., Lucas, R. M., Kuto, E., Gueye, Y., and Ndiaye, L.: Global Mangrove Watch: Monthly Alerts of Mangrove Loss for Africa, *Remote Sens-Basel*, 15, 2050, <https://doi.org/10.3390/rs15082050>, 2023.
- 915 Bunting, P., Rosenqvist, A., Hilarides, L., Lucas, R. M., Thomas, N., Tadono, T., Worthington, T. A., Spalding, M., Murray, N. J., and Rebelo, L. M.: Global Mangrove Extent Change 1996-2020: Global Mangrove Watch Version 3.0, *Remote Sens-Basel*, 14, <https://doi.org/10.3390/rs14153657>, 2022.



- Bunting, P., Rosenqvist, A., Lucas, R. M., Rebelo, L. M., Hilarides, L., Thomas, N., Hardy, A., Itoh, T., Shimada, M., and  
920 Finlayson, C. M.: The Global Mangrove Watch — A New 2010 Global Baseline of Mangrove Extent, *Remote Sens-  
Basel*, 10, 1669, <https://doi.org/10.3390/rs10101669>, 2018.
- Bwangoy, J. R. B., Hansen, M. C., Roy, D. P., De Grandi, G., and Justice, C. O.: Wetland mapping in the Congo Basin using  
optical and radar remotely sensed data and derived topographical indices, *Remote Sens. Environ.*, 114, 73-86,  
<https://doi.org/10.1016/j.rse.2009.08.004>, 2010.
- 925 Campbell, D.: The Congo River basin, in: *The World's Largest Wetlands: Ecology and Conservation*, edited by: Fraser, L. H.  
and Keddy, P. A., Cambridge University Press, Cambridge, 149-165, <https://doi.org/10.1017/CBO9780511542091.006>,  
2005.
- Cheng, F. Y., Van Meter, K. J., Byrnes, D. K., and Basu, N. B.: Maximizing US nitrate removal through wetland protection  
and restoration, *Nature*, 588, 625-630, <https://doi.org/10.1038/s41586-020-03042-5>, 2020.
- 930 Chmura, G. L., Anisfeld, S. C., Cahoon, D. R., and Lynch, J. C.: Global carbon sequestration in tidal, saline wetland soils,  
*Global Biogeochem. Cy.*, 17, 1111, <https://doi.org/10.1029/2002gb001917>, 2003.
- Cízková, H., Kvet, J., Comín, F. A., Laiho, R., Pokorný, J., and Pithart, D.: Actual state of European wetlands and their  
possible future in the context of global climate change, *Aquat. Sci.*, 75, 3-26, [https://doi.org/10.1007/s00027-011-0233-  
4](https://doi.org/10.1007/s00027-011-0233-4), 2013.
- 935 Cohen, M. J., Creed, I. F., Alexander, L., Basu, N. B., Calhoun, A. J. K., Craft, C., D'Amico, E., DeKeyser, E., Fowler, L.,  
Golden, H. E., Jawitz, J. W., Kalla, P., Kirkman, L. K., Lane, C. R., Lang, M., Leibowitz, S. G., Lewis, D. B., Marton,  
J., McLaughlin, D. L., Mushet, D. M., Raanan-Kiperwas, H., Rains, M. C., Smith, L., and Walls, S. C.: Do  
geographically isolated wetlands influence landscape functions?, *P. Natl. Acad. Sci. USA*, 113, 1978-1986,  
<https://doi.org/10.1073/pnas.1512650113>, 2016.
- 940 Cooley, S. W., Ryan, J. C., and Smith, L. C.: Human alteration of global surface water storage variability, *Nature*, 591, 78-  
81, <https://doi.org/10.1038/s41586-021-03262-3>, 2021.
- Costanza, R., d'Arge, R., de Groot, R., Farber, S., Grasso, M., Hannon, B., Limburg, K., Naeem, S., O'Neill, R. V., Paruelo,  
J., Raskin, R. G., Sutton, P., and van den Belt, M.: The value of the world's ecosystem services and natural capital, *Ecol.  
Econ.*, 25, 3-15, [https://doi.org/10.1016/s0921-8009\(98\)00020-2](https://doi.org/10.1016/s0921-8009(98)00020-2), 1998.
- 945 Cowardin, L. M. and Golet, F. C.: US Fish and Wildlife Service 1979 wetland classification: A review, in: *Classification and  
Inventory of the World's Wetlands*, edited by: Finlayson, C. M., and van der Valk, A. G., Springer Netherlands,  
Dordrecht, 139-152, [https://doi.org/10.1007/978-94-011-0427-2\\_12](https://doi.org/10.1007/978-94-011-0427-2_12), 1995.
- Cowardin, L. M., Carter, V., Golet, F. C., and LaRoe, E. T.: Classification of wetlands and deepwater habitats of the United  
States, Fish and Wildlife Service, US Department of the Interior, Washington, DC,  
950 [https://www.epa.gov/sites/default/files/2017-05/documents/cowardin\\_1979.pdf](https://www.epa.gov/sites/default/files/2017-05/documents/cowardin_1979.pdf), 1979.



- Dahl, T. E.: Status and Trends of Wetlands in the Conterminous United States 2004 to 2009, US Department of the Interior, Fisheries and Wildlife Service, Washington, DC., 108 pp., <https://www.fws.gov/sites/default/files/documents/Status-and-Trends-of-Wetlands-in-the-Conterminous-United-States-2004-to-2009.pdf>, 2011.
- 955 Dallaire, C. O., Lehner, B., Sayre, R., and Thieme, M.: A multidisciplinary framework to derive global river reach classifications at high spatial resolution, *Environ. Res. Lett.*, 14, 024003, <https://doi.org/10.1088/1748-9326/aad8e9>, 2019.
- Dargie, G. C., Lewis, S. L., Lawson, I. T., Mitchard, E. T. A., Page, S. E., Bocko, Y. E., and Ifo, S. A.: Age, extent and carbon storage of the central Congo Basin peatland complex, *Nature*, 542, 86-90, <https://doi.org/10.1038/nature21048>, 2017.
- 960 Darrah, S. E., Shennan-Farpon, Y., Loh, J., Davidson, N. C., Finlayson, C. M., Gardner, R. C., and Walpole, M. J.: Improvements to the Wetland Extent Trends (WET) index as a tool for monitoring natural and human-made wetlands, *Ecol. Indic.*, 99, 294-298, <https://doi.org/10.1016/j.ecolind.2018.12.032>, 2019.
- Davidson, N. C. and Finlayson, C. M.: Extent, regional distribution and changes in area of different classes of wetland, *Mar. Freshwater Res.*, 69, 1525-1533, <https://doi.org/10.1071/mf17377>, 2018.
- 965 Davidson, N. C., Fluet-Chouinard, E., and Finlayson, C. M.: Global extent and distribution of wetlands: trends and issues, *Mar. Freshwater Res.*, 69, 620-627, <https://doi.org/10.1071/mf17019>, 2018.
- Davis, C. A., Dvoretz, D., and Bidwell, J. R.: Hydrogeomorphic classification and functional assessment, in: *Wetland Techniques: Volume 3: Applications and Management*, edited by: Anderson, J. T., and Davis, C. A., 29-68, [https://doi.org/10.1007/978-94-007-6907-6\\_2](https://doi.org/10.1007/978-94-007-6907-6_2), 2013.
- 970 Ding, M., Wang, J. D., Song, C. Q., Sheng, Y. W., Hutchinson, J. M. S., Langston, A. L., and Marston, L.: A framework of freshwater and saline lake typology classification through leveraging hydroclimate, spectral, and literature evidence, *J. Hydrol.*, 632, 130704, <https://doi.org/10.1016/j.jhydrol.2024.130704>, 2024.
- Downing, J. A., Cole, J. J., Duarte, C. M., Middelburg, J. J., Melack, J. M., Prairie, Y. T., Kortelainen, P., Striegl, R. G., McDowell, W. H., and Tranvik, L. J.: Global abundance and size distribution of streams and rivers, *Inland Waters*, 2, 975 229-236, <https://doi.org/10.5268/iw-2.4.502>, 2012.
- Downing, J. A., Prairie, Y. T., Cole, J. J., Duarte, C. M., Tranvik, L. J., Striegl, R. G., McDowell, W. H., Kortelainen, P., Caraco, N. F., and Melack, J. M.: The global abundance and size distribution of lakes, ponds, and impoundments, *Limnol. Oceanogr.*, 51, 2388-2397, <https://doi.org/10.4319/lo.2006.51.5.2388>, 2006.
- 980 Duarte, C. M., Middelburg, J. J., and Caraco, N.: Major role of marine vegetation on the oceanic carbon cycle, *Biogeosciences*, 2, 1-8, <https://doi.org/10.5194/bg-2-1-2005>, 2005.
- Dugan, P., Dugan, P., Bellamy, D., International Union for Conservation of Nature and Natural Resources, and Holdgate, M. W.: *Wetlands in Danger: A World Conservation Atlas*, Oxford University Press, ISBN 0195209427, 1993.
- Edmonds, D. A., Caldwell, R. L., Brondizio, E. S., and Siani, S. M. O.: Coastal flooding will disproportionately impact people on river deltas, *Nat. Commun.*, 11, 4741, <https://doi.org/10.1038/s41467-020-18531-4>, 2020.



- 985 Environment and Climate Change Canada: Canadian Environmental Sustainability Indicators: Extent of Canada's Wetlands, Government of Canada, <https://www.canada.ca/en/environment-climate-change/services/environmental-indicators/extent-wetlands.html>, 2016.
- Ericson, J. P., Vörösmarty, C. J., Dingman, S. L., Ward, L. G., and Meybeck, M.: Effective sea-level rise and deltas: Causes of change and human dimension implications, *Global Planet. Change*, 50, 63-82, <https://doi.org/10.1016/j.gloplacha.2005.07.004>, 2006.
- 990 Fan, Y. and Miguez-Macho, G.: A simple hydrologic framework for simulating wetlands in climate and earth system models, *Clim. Dynam.*, 37, 253-278, <https://doi.org/10.1007/s00382-010-0829-8>, 2011.
- FAOSTAT: Crops and Livestock Products [dataset], <https://www.fao.org/faostat/en/#data/QCL>, 2024.
- Federal Republic of Nigeria: National Rice Development Strategy (NRDS), National Food Reserve Agency (NFRA), 995 Federal Ministry of Agriculture & Water Resources, Japan International Cooperation Agency (JICA), 62 pp., [https://www.jica.go.jp/Resource/english/our\\_work/thematic\\_issues/agricultural/pdf/nigeria\\_en.pdf](https://www.jica.go.jp/Resource/english/our_work/thematic_issues/agricultural/pdf/nigeria_en.pdf), 2009.
- Finlayson, C. M.: Ramsar Convention Typology of Wetlands, in: *The Wetland Book: I: Structure and Function, Management and Methods*, edited by: Finlayson, C. M., Everard, M., Irvine, K., McInnes, R. J., Middleton, B. A., van Dam, A. A., and Davidson, N. C., Springer, Dordrecht, 1529-1532, [https://doi.org/10.1007/978-94-007-6172-8\\_339-1](https://doi.org/10.1007/978-94-007-6172-8_339-1), 1000 2016.
- Finlayson, C. M. and Davidson, N. C.: Summary report, in: *Global review of wetland resources and priorities for wetland inventory*, edited by: Finlayson, C. M., and Spiers, A. G., Supervising Scientist Report 144 / Wetlands International Publication 53, Canberra, 1-14, <https://www.dceew.gov.au/sites/default/files/documents/ssr144-full-report-web.pdf>, 1999.
- 1005 Fleischmann, A. S., Papa, F., Fassoni-Andrade, A., Melack, J. M., Wongchuig, S., Paiva, R. C. D., Hamilton, S. K., Fluet-Chouinard, E., Barbedo, R., Aires, F., Al Bitar, A., Bonnet, M. P., Coe, M., Ferreira-Ferreira, J., Hess, L., Jensen, K., McDonald, K., Ovando, A., Park, E., Parrens, M., Pinel, S., Prigent, C., Resende, A. F., Revel, M., Rosenqvist, A., Rosenqvist, J., Rudorff, C., Silva, T. S. F., Yamazaki, D., and Collischonn, W.: How much inundation occurs in the Amazon River basin?, *Remote Sens. Environ.*, 278, <https://doi.org/10.1016/j.rse.2022.113099>, 2022.
- 1010 Fluet-Chouinard, E., Lehner, B., Rebelo, L. M., Papa, F., and Hamilton, S. K.: Development of a global inundation map at high spatial resolution from topographic downscaling of coarse-scale remote sensing data, *Remote Sens. Environ.*, 158, 348-361, <https://doi.org/10.1016/j.rse.2014.10.015>, 2015.
- Fluet-Chouinard, E., Stocker, B. D., Zhang, Z., Malhotra, A., Melton, J. R., Poulter, B., Kaplan, J. O., Goldewijk, K. K., Siebert, S., Minayeva, T., Hugelius, G., Joosten, H., Barthelmes, A., Prigent, C., Aires, F., Hoyt, A. M., Davidson, N., 1015 Finlayson, C. M., Lehner, B., Jackson, R. B., and McIntyre, P. B.: Extensive global wetland loss over the past three centuries, *Nature*, 614, 281-286, <https://doi.org/10.1038/s41586-022-05572-6>, 2023.
- Gallant, A. L.: The Challenges of Remote Monitoring of Wetlands, *Remote Sens-Basel*, 7, 10938-10950, <https://doi.org/10.3390/rs70810938>, 2015.





- 1020 Gedan, K. B., Kirwan, M. L., Wolanski, E., Barbier, E. B., and Silliman, B. R.: The present and future role of coastal wetland vegetation in protecting shorelines: answering recent challenges to the paradigm, *Climate Change*, 106, 7-29, <https://doi.org/10.1007/s10584-010-0003-7>, 2011.
- 1025 Gerbeaux, P., Finlayson, C. M., and van Dam, A. A.: Wetland Classification: Overview, in: *The Wetland Book: I: Structure and Function, Management and Methods*, edited by: Finlayson, C. M., Everard, M., Irvine, K., McInnes, R. J., Middleton, B. A., van Dam, A. A., and Davidson, N., Springer, Dordrecht, 1-8, [https://doi.org/10.1007/978-94-007-6172-8\\_329-1](https://doi.org/10.1007/978-94-007-6172-8_329-1), 2016.
- Gibbs, J. P.: Wetland loss and biodiversity conservation, *Conserv. Biol.*, 14, 314-317, <https://doi.org/10.1046/j.1523-1739.2000.98608.x>, 2000.
- 1030 Giri, C., Ochieng, E., Tieszen, L. L., Zhu, Z., Singh, A., Loveland, T., Masek, J., and Duke, N.: Status and distribution of mangrove forests of the world using earth observation satellite data, *Global. Ecol. Biogeogr.*, 20, 154-159, <https://doi.org/10.1111/j.1466-8238.2010.00584.x>, 2011.
- Gourcy, L., Aranyosy, J.-F., Olivry, J.-C., and Zuppi, G. M.: Évolution spatio-temporelle des teneurs isotopiques ( $\delta^2\text{H}$ – $\delta^{18}\text{O}$ ) des eaux de la cuvette lacustre du fleuve Niger (Mali), *C. R. Acad. Sci. II A*, 331, 701-707, [https://doi.org/10.1016/S1251-8050\(02\)90003-0](https://doi.org/10.1016/S1251-8050(02)90003-0), 2000.
- 1035 Government of India: Economic Survey 2022-23 Statistical Appendix, <https://www.indiabudget.gov.in/economicsurvey/doc/Statistical-Appendix-in-English.pdf>, 2023.
- Gumbricht, T., Roman-Cuesta, R. M., Verchot, L., Herold, M., Wittmann, F., Householder, E., Herold, N., and Murdiyarso, D.: An expert system model for mapping tropical wetlands and peatlands reveals South America as the largest contributor, *Glob. Change Biol.*, 23, 3581-3599, <https://doi.org/10.1111/gcb.13689>, 2017.
- 1040 Hansen, M. C., Potapov, P. V., Moore, R., Hancher, M., Turubanova, S. A., Tyukavina, A., Thau, D., Stehman, S. V., Goetz, S. J., Loveland, T. R., Kommareddy, A., Egorov, A., Chini, L., Justice, C. O., and Townshend, J. R. G.: High-Resolution Global Maps of 21st-Century Forest Cover Change, *Science*, 342, 850-853, <https://doi.org/10.1126/science.1244693>, 2013.
- 1045 Hengl, T., de Jesus, J. M., Heuvelink, G. B. M., Gonzalez, M. R., Kilibarda, M., Blagotic, A., Shangquan, W., Wright, M. N., Geng, X. Y., Bauer-Marschallinger, B., Guevara, M. A., Vargas, R., MacMillan, R. A., Batjes, N. H., Leenaars, J. G. B., Ribeiro, E., Wheeler, I., Mantel, S., and Kempen, B.: SoilGrids250m: Global gridded soil information based on machine learning, *Plos One*, 12, <https://doi.org/10.1371/journal.pone.0169748>, 2017.
- Hu, S. J., Niu, Z. G., and Chen, Y. F.: Global Wetland Datasets: a Review, *Wetlands*, 37, 807-817, <https://doi.org/10.1007/s13157-017-0927-z>, 2017a.
- 1050 Hu, S. J., Niu, Z. G., Chen, Y. F., Li, L. F., and Zhang, H. Y.: Global wetlands: Potential distribution, wetland loss, and status, *Sci. Total Environ.*, 586, 319-327, <https://doi.org/10.1016/j.scitotenv.2017.02.001>, 2017b.
- Hugelius, G., Loisel, J., Chadburn, S., Jackson, R. B., Jones, M., MacDonald, G., Marushchak, M., Olefeldt, D., Packalen, M., Siewert, M. B., Treat, C., Turetsky, M., Voigt, C., and Yu, Z. C.: Large stocks of peatland carbon and nitrogen are



- vulnerable to permafrost thaw, P. Natl. Acad. Sci. USA, 117, 20438-20446, <https://doi.org/10.1073/pnas.1916387117>, 2020.
- 1055 Jensen, K. and McDonald, K.: Surface Water Microwave Product Series Version 3: A Near-Real Time and 25-Year Historical Global Inundated Area Fraction Time Series From Active and Passive Microwave Remote Sensing, IEEE Geosci. Remote S., 16, 1402-1406, <https://doi.org/10.1109/lgrs.2019.2898779>, 2019.
- Joosten, H.: The Global Peatland CO<sub>2</sub> Picture: peatland status and drainage related emissions in all countries of the world, Greifswald University, Wetlands International, <https://www150.statcan.gc.ca/n1/pub/16-001-m/16-001-m2022001-eng.htm>, 2009.
- 1060 Junk, W. J., An, S. Q., Finlayson, C. M., Gopal, B., Kvet, J., Mitchell, S. A., Mitsch, W. J., and Robarts, R. D.: Current state of knowledge regarding the world's wetlands and their future under global climate change: a synthesis, Aquat. Sci., 75, 151-167, <https://doi.org/10.1007/s00027-012-0278-z>, 2013.
- Keith, D. A., Ferrer-Paris, J. R., Nicholson, E., Bishop, M. J., Polidoro, B. A., Ramirez-Llodra, E., Tozer, M. G., Nel, J. L., 1065 Mac Nally, R., Gregr, E. J., Watermeyer, K. E., Essl, F., Faber-Langendoen, D., Franklin, J., Lehmann, C. E. R., Etter, A., Roux, D. J., Stark, J. S., Rowland, J. A., Brummitt, N. A., Fernandez-Arcaya, U. C., Suthers, I. M., Wisser, S. K., Donohue, I., Jackson, L. J., Pennington, R. T., Iliffe, T. M., Gerovasileiou, V., Giller, P., Robson, B. J., Pettorelli, N., Andrade, A., Lindgaard, A., Tahvanainen, T., Terauds, A., Chadwick, M. A., Murray, N. J., Moat, J., Plissock, P., Zager, I., and Kingsford, R. T.: A function-based typology for Earth's ecosystems, Nature, 610, 513-518, 1070 <https://doi.org/10.1038/s41586-022-05318-4>, 2022.
- Laborte, A. G., Gutierrez, M. A., Balanza, J. G., Saito, K., Zwart, S. J., Boschetti, M., Murty, M. V. R., Villano, L., Aunario, J. K., Reinke, R., Koo, J., Hijmans, R. J., and Nelson, A.: RiceAtlas, a spatial database of global rice calendars and production, Scientific Data, 4, 170074, <https://doi.org/10.1038/sdata.2017.74>, 2017.
- Lane, C. R., D'Amico, E., Christensen, J. R., Golden, H. E., Wu, Q. S., and Rajib, A.: Mapping global non-floodplain 1075 wetlands, Earth Syst. Sci. Data, 15, 2927-2955, <https://doi.org/10.5194/essd-15-2927-2023>, 2023.
- Lehner, B. and Döll, P.: Development and validation of a global database of lakes, reservoirs and wetlands, J. Hydrol., 296, 1-22, <https://doi.org/10.1016/j.jhydrol.2004.03.028>, 2004.
- Lehner, B., Anand, M., Fluet-Chouinard, E., Tan, F., Aires, F., Allen, G. H., Bousquet, P., Canadell, J. G., Davidson, N., Finlayson, C. M., Gumbricht, T., Hilarides, L., Hugelius, G., Jackson, R. B., Korver, M. C., McIntyre, P. B., Nagy, S., 1080 Olefeldt, D., Pavelsky, T. M., Pekel, J.-F., Poulter, B., Prigent, C., Wang, J., Worthington, T. A., Yamazaki, D., Thieme, M.: Global Lakes and Wetlands Database (GLWD) version 2.0 [dataset], <https://figshare.com/s/e40017f69f41f80d50df>, 2024.
- Lehner, B., Beames, P., Mulligan, M., Zarfl, C., De Felice, L., van Soesbergen, A., Thieme, M., Garcia de Leaniz, C., Anand, M., Belletti, B., Brauman, K. A., Januchowski-Hartley, S. R., Lyon, K., Mandle, L., Mazany-Wright, N., 1085 Messenger, M. L., Pavelsky, T., Pekel, J.-F., Wang, J., Wen, Q., Wishart, M., Xing, T., Yang, X., and Higgins, J.: The



- Global Dam Watch database of river barrier and reservoir information for large-scale applications, *Scientific Data*, in review.
- Lehner, B., Liermann, C. R., Revenga, C., Vörösmarty, C., Fekete, B., Crouzet, P., Döll, P., Endejan, M., Frenken, K., Magome, J., Nilsson, C., Robertson, J. C., Rödel, R., Sindorf, N., and Wisser, D.: High-resolution mapping of the world's reservoirs and dams for sustainable river-flow management, *Front. Ecol. Environ.*, 9, 494-502, <https://doi.org/10.1890/100125>, 2011.
- Lehner, B., Messenger, M. L., Korver, M. C., and Linke, S.: Global hydro-environmental lake characteristics at high spatial resolution, *Scientific Data*, 9, <https://doi.org/10.1038/s41597-022-01425-z>, 2022.
- Lieth, H.: Primary Production of the Major Vegetation Units of the World, in: *Primary Productivity of the Biosphere*, edited by: Lieth, H., and Whittaker, R. H., *Ecological Studies*, Springer, Berlin, Heidelberg, 203-215, [https://doi.org/10.1007/978-3-642-80913-2\\_10](https://doi.org/10.1007/978-3-642-80913-2_10), 1975.
- Lindersson, S., Brandimarte, L., Mard, J., and Di Baldassarre, G.: A review of freely accessible global datasets for the study of floods, droughts and their interactions with human societies, *Wiley Interdisciplinary Reviews-Water*, 7, <https://doi.org/10.1002/wat2.1424>, 2020.
- Linke, S., Lehner, B., Dallaire, C. O., Ariwi, J., Grill, G., Anand, M., Beames, P., Burchard-Levine, V., Maxwell, S., Moidu, H., Tan, F., and Thieme, M.: Global hydro-environmental sub-basin and river reach characteristics at high spatial resolution, *Scientific Data*, 6, <https://doi.org/10.1038/s41597-019-0300-6>, 2019.
- Mahdavi, S., Salehi, B., Granger, J., Amani, M., Brisco, B., and Huang, W. M.: Remote sensing for wetland classification: a comprehensive review, *Gisci. Remote Sens.*, 55, 623-658, <https://doi.org/10.1080/15481603.2017.1419602>, 2018.
- Marconcini, M., Metz-Marconcini, A., Esch, T., and Gorelick, N.: Understanding Current Trends in Global Urbanisation - The World Settlement Footprint Suite, *GI\_Forum*, 33-38, [https://doi.org/10.1553/giscience2021\\_01\\_s33](https://doi.org/10.1553/giscience2021_01_s33), 2021.
- Marois, D. E. and Mitsch, W. J.: Coastal protection from tsunamis and cyclones provided by mangrove wetlands – a review, *International Journal of Biodiversity Science, Ecosystem Services & Management*, 11, 71-83, <https://doi.org/10.1080/21513732.2014.997292>, 2015.
- Matthews, E. and Fung, I.: Methane Emission from Natural Wetlands: Global distribution, area, and Environmental Characteristics of Sources, *Global Biogeochem. Cy.*, 1, 61-86, <https://doi.org/10.1029/GB001i001p00061>, 1987.
- McCarthy, J. M., Gumbrecht, T., McCarthy, T., Frost, P., Wessels, K., and Seidel, F.: Flooding patterns of the Okavango wetland in Botswana between 1972 and 2000, *Ambio*, 32, 453-457, [https://doi.org/10.1639/0044-7447\(2003\)032\[0453:Fpotow\]2.0.Co;2](https://doi.org/10.1639/0044-7447(2003)032[0453:Fpotow]2.0.Co;2), 2003.
- Mcowen, C. J., Weatherdon, L. V., Van Bochove, J. W., Sullivan, E., Blyth, S., Zockler, C., Stanwell-Smith, D., Kingston, N., Martin, C. S., Spalding, M., and Fletcher, S.: A global map of saltmarshes, *Biodiversity Data Journal*, 5, <https://doi.org/10.3897/BDJ.5.e11764>, 2017.
- Melton, J. R., Wania, R., Hodson, E. L., Poulter, B., Ringeval, B., Spahni, R., Bohn, T., Avis, C. A., Beerling, D. J., Chen, G., Eliseev, A. V., Denisov, S. N., Hopcroft, P. O., Lettenmaier, D. P., Riley, W. J., Singarayer, J. S., Subin, Z. M.,



- 1120 Tian, H., Zürcher, S., Brovkin, V., van Bodegom, P. M., Kleinen, T., Yu, Z. C., and Kaplan, J. O.: Present state of global wetland extent and wetland methane modelling: conclusions from a model inter-comparison project (WETCHIMP), *Biogeosciences*, 10, 753-788, <https://doi.org/10.5194/bg-10-753-2013>, 2013.
- Messenger, M. L., Lehner, B., Cockburn, C., Lamouroux, N., Pella, H., Snelder, T., Tockner, K., Trautmann, T., Watt, C., and Detry, T.: Global prevalence of non-perennial rivers and streams, *Nature*, 594, 391-397, <https://doi.org/10.1038/s41586-021-03565-5>, 2021.
- 1125 Messenger, M. L., Lehner, B., Grill, G., Nedeva, I., and Schmitt, O.: Estimating the volume and age of water stored in global lakes using a geo-statistical approach, *Nat. Commun.*, 7, <https://doi.org/10.1038/ncomms13603>, 2016.
- Millennium Ecosystem Assessment: Ecosystems and Human Well-being: Wetlands and Water, Synthesis, World Resources Institute, Washington, DC, 80 pp., <https://www.millenniumassessment.org/documents/document.358.aspx.pdf>, 2005.
- 1130 Mitchell, S. A.: The status of wetlands, threats and the predicted effect of global climate change: the situation in Sub-Saharan Africa, *Aquat. Sci.*, 75, 95-112, <https://doi.org/10.1007/s00027-012-0259-2>, 2013.
- Mitsch, W. J. and Gosselink, J. G.: *Wetlands*, 5th edition, John Wiley & Sons., ISBN 9781119019787, 2015.
- Mitsch, W. J., Bernal, B., and Hernandez, M. E.: Ecosystem services of wetlands, *International Journal of Biodiversity Science, Ecosystem Services & Management*, 11, 1-4, <https://doi.org/10.1080/21513732.2015.1006250>, 2015.
- 1135 Mohamed, Y. A., Bastiaanssen, W. G. M., and Savenije, H. H. G.: Spatial variability of evaporation and moisture storage in the swamps of the upper Nile studied by remote sensing techniques, *J. Hydrol.*, 289, 145-164, <https://doi.org/10.1016/j.jhydrol.2003.11.038>, 2004.
- Muis, S., Apecechea, M. I., Álvarez, J.A., Verlaan, M., Yan, K., Dullaart, J., Aerts, J., Duong, T., Ranasinghe, R., le Bars, D., Haarsma, R., Roberts, M.: Global sea level change indicators from 1950 to 2050 derived from reanalysis and high resolution CMIP6 climate projections. Copernicus Climate Change Service (C3S) Climate Data Store (CDS). <https://doi.org/10.24381/cds.6edf04e0>, 2022.
- 1140 Mulatu, D. W., Ahmed, J., Semereab, E., Arega, T., Yohannes, T., and Akwany, L. O.: Stakeholders, Institutional Challenges and the Valuation of Wetland Ecosystem Services in South Sudan: The Case of Machar Marshes and Sudd Wetlands. *Environ. Manage.*, 69, 666-683, <https://doi.org/10.1007/s00267-022-01609-8>, 2022.
- 1145 Mulholland, P. J. and Elwood, J. W.: The role of lake and reservoir sediments as sinks in the perturbed global carbon cycle, *Tellus*, 34, 490-499, <https://doi.org/10.3402/tellusa.v34i5.10834>, 1982.
- Murray, N. J., Phinn, S. R., DeWitt, M., Ferrari, R., Johnston, R., Lyons, M. B., Clinton, N., Thau, D., and Fuller, R. A.: The global distribution and trajectory of tidal flats, *Nature*, 565, 222-225, <https://doi.org/10.1038/s41586-018-0805-8>, 2019.
- Murray, N. J., Worthington, T. A., Bunting, P., Duce, S., Hagger, V., Lovelock, C. E., Lucas, R., Saunders, M. I., Sheaves, M., Spalding, M., Waltham, N. J., and Lyons, M. B.: High-resolution mapping of losses and gains of Earth's tidal wetlands, *Science*, 376, 744-749, <https://doi.org/10.1126/science.abm9583>, 2022.
- 1150 Najjar, R. G., Herrmann, M., Alexander, R., Boyer, E. W., Burdige, D. J., Butman, D., Cai, W. J., Canuel, E. A., Chen, R. F., Friedrichs, M. A. M., Feagin, R. A., Griffith, P. C., Hinson, A. L., Holmquist, J. R., Hu, X., Kemp, W. M., Kroeger, K.



- D., Mannino, A., McCallister, S. L., McGillis, W. R., Mulholland, M. R., Pilskaln, C. H., Salisbury, J., Signorini, S. R.,  
1155 St-Laurent, P., Tian, H., Tzortziou, M., Vlahos, P., Wang, Z. A., and Zimmerman, R. C.: Carbon Budget of Tidal  
Wetlands, Estuaries, and Shelf Waters of Eastern North America, *Global Biogeochem. Cy.*, 32, 389-416,  
<https://doi.org/10.1002/2017gb005790>, 2018.
- Nakaegawa, T.: Comparison of Water-Related Land Cover Types in Six 1-km Global Land Cover Datasets, *J.*  
*Hydrometeorol.*, 13, 649-664, <https://doi.org/10.1175/jhm-d-10-05036.1>, 2012.
- 1160 National Bureau of Statistics of China: 年度数据 [annual data] [dataset],  
<https://data.stats.gov.cn/easyquery.htm?cn=C01&zb=A0D0E&sj=last12>, 2023.
- Nicholls, R. J., Hoozemans, F. M. J., and Marchand, M.: Increasing flood risk and wetland losses due to global sea-level  
rise: regional and global analyses, *Global Environ. Chang.*, 9, S69-S87, [https://doi.org/10.1016/s0959-3780\(99\)00019-9](https://doi.org/10.1016/s0959-3780(99)00019-9),  
1999.
- 1165 Nivet, C. and Frazier, S.: A review of European wetland inventory information, Wetlands International, Wageningen, 2004.
- Olefeldt, D., Hovemyr, M., Kuhn, M. A., Bastviken, D., Bohn, T. J., Connolly, J., Crill, P., Euskirchen, E. S., Finkelstein, S.  
A., Genet, H., Grosse, G., Harris, L. I., Heffernan, L., Helbig, M., Hugelius, G., Hutchins, R., Juutinen, S., Lara, M. J.,  
Malhotra, A., Manies, K., McGuire, A. D., Natali, S. M., O'Donnell, J. A., Parmentier, F. J. W., Räsänen, A., Schädel,  
C., Sonnentag, O., Strack, M., Tank, S. E., Treat, C., Varner, R. K., Virtanen, T., Warren, R. K., and Watts, J. D.: The  
1170 Boreal-Arctic Wetland and Lake Dataset (BAWLD), *Earth Syst. Sci. Data*, 13, 5127-5149, <https://doi.org/10.5194/essd-13-5127-2021>, 2021.
- Page, S. E., Rieley, J. O., and Banks, C. J.: Global and regional importance of the tropical peatland carbon pool, *Glob.*  
*Change Biol.*, 17, 798-818, <https://doi.org/10.1111/j.1365-2486.2010.02279.x>, 2011.
- Pekel, J. F., Cottam, A., Gorelick, N., and Belward, A. S.: High-resolution mapping of global surface water and its long-term  
1175 changes, *Nature*, 540, 418-422, <https://doi.org/10.1038/nature20584>, 2016.
- Pendleton, L., Donato, D. C., Murray, B. C., Crooks, S., Jenkins, W. A., Sifleet, S., Craft, C., Fourqurean, J. W., Kauffman,  
J. B., Marbà, N., Megonigal, P., Pidgeon, E., Herr, D., Gordon, D., and Baldera, A.: Estimating Global "Blue Carbon"  
Emissions from Conversion and Degradation of Vegetated Coastal Ecosystems, *Plos One*, 7,  
<https://doi.org/10.1371/journal.pone.0043542>, 2012.
- 1180 Pi, X. H., Luo, Q. Q., Feng, L., Xu, Y., Tang, J., Liang, X. Y., Ma, E. Z., Cheng, R., Fensholt, R., Brandt, M., Cai, X. B.,  
Gibson, L., Liu, J. G., Zheng, C. M., Li, W. F., and Bryan, B. A.: Mapping global lake dynamics reveals the emerging  
roles of small lakes, *Nat. Commun.*, 13, <https://doi.org/10.1038/s41467-022-33239-3>, 2022.
- Pickens, A. H., Hansen, M. C., Hancher, M., Stehman, S. V., Tyukavina, A., Potapov, P., Marroquin, B., and Sherani, Z.:  
Mapping and sampling to characterize global inland water dynamics from 1999 to 2018 with full Landsat time-series,  
1185 *Remote Sens. Environ.*, 243, <https://doi.org/10.1016/j.rse.2020.111792>, 2020.
- Poffenbarger, H. J., Needelman, B. A., and Megonigal, J. P.: Salinity Influence on Methane Emissions from Tidal Marshes,  
*Wetlands*, 31, 831-842, <https://doi.org/10.1007/s13157-011-0197-0>, 2011.



- Portmann, F. T., Siebert, S., and Döll, P.: MIRCA2000-Global monthly irrigated and rainfed crop areas around the year 2000: A new high-resolution data set for agricultural and hydrological modeling, *Global Biogeochem. Cy.*, 24, <https://doi.org/10.1029/2008gb003435>, 2010.
- Prigent, C. and Papa, F.: Multisatellite Remote Sensing of Global Wetland Extent and Dynamics, in: *Remote Sensing of Wetlands: Applications and Advances*, 1st ed., edited by: Tiner, R. W., Lang, M. W., and Klemas, V. V., CRC Press, 511-526, ISBN 9780429183294, 2015.
- Prigent, C., Jimenez, C., and Bousquet, P.: Satellite-Derived Global Surface Water Extent and Dynamics Over the Last 25 Years (GIEMS-2), *J. Geophys. Res-Atmos.*, 125, <https://doi.org/10.1029/2019jd030711>, 2020.
- Prigent, C., Papa, F., Aires, F., Rossow, W. B., and Matthews, E.: Global inundation dynamics inferred from multiple satellite observations, 1993-2000, *J. Geophys. Res-Atmos.*, 112, <https://doi.org/10.1029/2006jd007847>, 2007.
- Qiu, C. J., Ciais, P., Zhu, D., Guenet, B., Peng, S. S., Petrescu, A. M. R., Lauerwald, R., Makowski, D., Gallego-Sala, A. V., Charman, D. J., and Brewer, S. C.: Large historical carbon emissions from cultivated northern peatlands, *Science Advances*, 7, <https://doi.org/10.1126/sciadv.abf1332>, 2021.
- Rabinowitz, T. R. M. and Andrews, J.: Valuing the salt marsh ecosystem: Developing ecosystem accounts, <https://www150.statcan.gc.ca/n1/pub/16-001-m/16-001-m2022001-eng.htm>, 2022.
- Ramsar Convention on Wetlands: Convention on Wetlands of International Importance Especially as Waterfowl Habitat. Final Text adopted by the International Conference on the Wetlands and Waterfowl at Ramsar, Iran, 2 February 1971, Iran, [https://www.ramsar.org/sites/default/files/documents/library/original\\_1971\\_convention\\_e.pdf](https://www.ramsar.org/sites/default/files/documents/library/original_1971_convention_e.pdf), 1971.
- Ramsar Convention on Wetlands: Resolution VIII.6: A Ramsar Framework for Wetland Inventory, *Wetlands: water, life, and culture*, 8th Meeting of the Conference of the Contracting Parties to the Convention on Wetlands (Ramsar, Iran, 1971), 40 pp., [https://www.ramsar.org/sites/default/files/documents/library/key\\_res\\_viii\\_06\\_e.pdf](https://www.ramsar.org/sites/default/files/documents/library/key_res_viii_06_e.pdf), 2002
- Ramsar Convention on Wetlands: Global Wetland Outlook: Special Edition 2021, Gland, Switzerland: Secretariat of the Convention on Wetlands, <https://www.global-wetland-outlook.ramsar.org/report-1>, 2021.
- Ramsar: Delta Intérieur du Niger, <https://rsis.ramsar.org/ris/1365>, 2004.
- Ramsar: Sudd, <https://rsis.ramsar.org/ris/1622>, 2006.
- Ramsar: Hawizeh Marsh, <https://rsis.ramsar.org/ris/1718>, 2012.
- Ramsar: Central Marshes, <https://rsis.ramsar.org/ris/2241>, 2015a.
- Ramsar: Hammar Marsh, <https://rsis.ramsar.org/ris/2242>, 2015b.
- Raup, B., Racoviteanu, A., Khalsa, S. J. S., Helm, C., Armstrong, R., and Arnaud, Y.: The GLIMS geospatial glacier database: A new tool for studying glacier change, *Global Planet. Change*, 56, 101-110, <https://doi.org/10.1016/j.gloplacha.2006.07.018>, 2007.
- Raymond, P. A., Hartmann, J., Lauerwald, R., Sobek, S., McDonald, C., Hoover, M., Butman, D., Striegl, R., Mayorga, E., Humborg, C., Kortelainen, P., Dürr, H., Meybeck, M., Ciais, P., and Guth, P.: Global carbon dioxide emissions from inland waters, *Nature*, 503, 355-359, <https://doi.org/10.1038/nature12760>, 2013.





- Reis, V., Hermoso, V., Hamilton, S. K., Ward, D., Fluet-Chouinard, E., Lehner, B., and Linke, S.: A Global Assessment of Inland Wetland Conservation Status, *Bioscience*, 67, 523-533, <https://doi.org/10.1093/biosci/bix045>, 2017.
- Richardson, C. J. and Hussain, N. A.: Restoring the Garden of Eden: An ecological assessment of the marshes of Iraq, *Bioscience*, 56, 477-489, [https://doi.org/10.1641/0006-3568\(2006\)56\[477:Rtgoea\]2.0.Co;2](https://doi.org/10.1641/0006-3568(2006)56[477:Rtgoea]2.0.Co;2), 2006.
- 1225
- Rosegrant, M. W., Cai, X., Cline, S. A., and Nakagawa, N.: The role of rainfed agriculture in the future of global food production, International Food Policy Research Institute (IFPRI), Washington, DC, 105 pp., 2002.
- Salmon, J. M., Friedl, M. A., Frohling, S., Wisser, D., and Douglas, E. M.: Global rain-fed, irrigated, and paddy croplands: A new high resolution map derived from remote sensing, crop inventories and climate data, *Int. J. Appl. Earth Obs.*, 38, 321-334, <https://doi.org/10.1016/j.jag.2015.01.014>, 2015.
- 1230
- Sanderman, J., Hengl, T., Fiske, G., Solvik, K., Adame, M. F., Benson, L., Bukoski, J. J., Carnell, P., Cifuentes-Jara, M., Donato, D., Duncan, C., Eid, E. M., zu Ermgassen, P., Lewis, C. J. E., Macreadie, P. I., Glass, L., Gress, S., Jardine, S. L., Jones, T. G., Nsombo, E. N., Rahman, M. M., Sanders, C. J., Spalding, M., and Landis, E.: A global map of mangrove forest soil carbon at 30 m spatial resolution, *Environ. Res. Lett.*, 13, <https://doi.org/10.1088/1748-9326/aabe1c>, 2018.
- 1235
- Saunio, M., Stavert, A. R., Poulter, B., Bousquet, P., Canadell, J. G., Jackson, R. B., Raymond, P. A., Dlugokencky, E. J., Houweling, S., Patra, P. K., Ciais, P., Arora, V. K., Bastviken, D., Bergamaschi, P., Blake, D. R., Brailsford, G., Bruhwiler, L., Carlson, K. M., Carrol, M., Castaldi, S., Chandra, N., Crevoisier, C., Crill, P. M., Covey, K., Curry, C. L., Etiope, G., Frankenberg, C., Gedney, N., Hegglin, M., Hoglund-Isaksson, L., Hugelius, G., Ishizawa, M., Ito, A., Janssens-Maenhout, G., Jensen, K. M., Joos, F., Kleinen, T., Krummel, P. B., Langenfelds, R. L., Laruelle, G. G., Liu, L. C., Machida, T., Maksyutov, S., McDonald, K. C., McNorton, J., Miller, P. A., Melton, J. R., Morino, I., Müller, J., Murguía-Flores, F., Naik, V., Niwa, Y., Noce, S., Doherty, S. O., Parker, R. J., Peng, C. H., Peng, S. S., Peters, G. P., Prigent, C., Prinn, R., Ramonet, M., Regnier, P., Riley, W. J., Rosentreter, J. A., Segers, A., Simpson, I. J., Shi, H., Smith, S. J., Steele, L. P., Thornton, B. F., Tian, H. Q., Tohjima, Y., Tubiello, F. N., Tsuruta, A., Viovy, N., Voulgarakis, A., Weber, T. S., van Weele, M., van der Werf, G. R., Weiss, R. F., Worthy, D., Wunch, D., Yin, Y., Yoshida, Y., Zhang, W. X., Zhang, Z., Zhao, Y. H., Zheng, B., Zhu, Q., Zhu, Q. A., and Zhuang, Q. L.: The Global Methane Budget 2000-2017, *Earth Syst. Sci. Data*, 12, 1561-1623, <https://doi.org/10.5194/essd-12-1561-2020>, 2020.
- 1240
- Sayre, R., Karagulle, D., Frye, C., Boucher, T., Wolff, N. H., Breyer, S., Wright, D., Martin, M., Butler, K., Van Graafeiland, K., Touval, J., Sotomayor, L., McGowan, J., Game, E. T., and Possingham, H.: An assessment of the representation of ecosystems in global protected areas using new maps of World Climate Regions and World Ecosystems, *Global Ecology and Conservation*, 21, <https://doi.org/10.1016/j.gecco.2019.e00860>, 2020.
- 1250
- Semeniuk, C. A. and Semeniuk, V.: A geomorphic approach to global classification for inland wetlands, *Vegetatio*, 118, 103-124, <https://doi.org/10.1007/bf00045193>, 1995.





- 1255 Semeniuk, C. A. and Semeniuk, V.: A comprehensive classification of inland wetlands of Western Australia using the geomorphic-hydrologic approach, *Journal of the Royal Society of Western Australia*, 94, 449, <https://archive.org/details/biostor-256347>, 2011.
- Semeniuk, V. and Semeniuk, C. A.: A geomorphic approach to global classification for natural inland wetlands and rationalization of the system used by the Ramsar Convention – a discussion, *Wetl. Ecol. Manag.*, 5, 145-158, <https://doi.org/10.1023/A:1008207726826>, 1997.
- 1260 Spalding, M., Kainuma, M., and Collins, L.: *World Atlas of Mangroves*, 1, London: Routledge., ISBN 9781844076574, 2010.
- Spiers, A. G.: Review of international/continental wetland resources, in: *Global review of wetland resources and priorities for wetland inventory*, edited by: Finlayson, C. M., and Spiers, A. G., Supervising Scientist Report 144 / Wetlands International Publication 53, Canberra, 63-104, <https://www.dccew.gov.au/sites/default/files/documents/ssr144-full-report-web.pdf>, 1999.
- 1265 Spiers, A. G.: Wetland inventory: Overview at a global scale, *Wetland inventory, assessment and monitoring: Practical techniques and identification of major issues.*, Dakar, Senegal, 8–14 November 1998, 23-30, <https://www.dccew.gov.au/sites/default/files/documents/ssr161.pdf>, 2001.
- Sun, Z. G., Sun, W. G., Tong, C., Zeng, C. S., Yu, X., and Mou, X. J.: China's coastal wetlands: Conservation history, 1270 implementation efforts, existing issues and strategies for future improvement, *Environ. Int.*, 79, 25-41, <https://doi.org/10.1016/j.envint.2015.02.017>, 2015.
- Sutcliffe, J. V. and Parks, Y. P.: Comparative balance of selected African wetlands, *Hydrolog. Sci. J.*, 34, 49-62, <https://doi.org/10.1080/02626668909491308>, 1989.
- Sutcliffe, J. V. and Parks, Y. P.: *The hydrology of the Nile*, Vol. 5, International Association of Hydrological Sciences 1275 Oxfordshire, UK, ISBN 9781901502756, 1999.
- Syvitski, J. P. M., Kettner, A. J., Overeem, I., Hutton, E. W. H., Hannon, M. T., Brakenridge, G. R., Day, J., Vörösmarty, C., Saito, Y., Giosan, L., and Nicholls, R. J.: Sinking deltas due to human activities, *Nat. Geosci.*, 2, 681-686, <https://doi.org/10.1038/ngco629>, 2009.
- Tallaksen, L. and van Lanen, H. A. J.: *Hydrological drought. Processes and estimation methods for streamflow and 1280 groundwater*, 2nd ed., *Developments in water science*, Elsevier, Amsterdam, <https://doi.org/10.1016/C2017-0-03464-X>, 2004.
- Tanneberger, F., Tegetmeyer, C., Busse, S., Barthelmes, A., Shumka, S., Marine, A. M., Jenderedjian, K., Steiner, G. M., Essl, F., Etzold, J., Mendes, C., Kozulin, A., Frankard, P., Milanovic, D., Ganeva, A., Apostolova, I., Alegro, A., Delipetrou, P., Navrátilová, J., Risager, M., Leivits, A., Fosaa, A. M., Tuominen, S., Muller, F., Bakuradze, T., Sommer, 1285 M., Christanis, K., Szurdoki, E., Oskarsson, H., Brink, S. H., Connolly, J., Bragazza, L., Martinelli, G., Aleksans, O., Priede, A., Sungaila, D., Melovski, L., Belous, T., Saveljic, D., de Vries, F., Moen, A., Dembek, W., Mateus, J., Hanganu, J., Sirin, A., Markina, A., Napreenko, M., Lazarevic, P., Stanová, V. S., Skoberne, P., Pérez, P. H.,



- Pontevedra-Pombal, X., Lonnstad, J., Kuchler, M., Wüst-Galley, C., Kirca, S., Mykytiuk, O., Lindsay, R., and Joosten, H.: The peatland map of Europe, *Mires Peat*, 19, <https://doi.org/10.19189/MaP.2016.OMB.264>, 2017.
- 1290 Tarnocai, C., Kettles, I. M., and Lacelle, B.: Peatlands of Canada; Geological Survey of Canada [dataset], <https://doi.org/10.4095/288786>, 2011.
- Tessler, Z. D., Vörösmarty, C. J., Grossberg, M., Gladkova, I., Aizenman, H., Syvitski, J. P. M., and Foufoula-Georgiou, E.: Profiling risk and sustainability in coastal deltas of the world, *Science*, 349, 638-643, <https://doi.org/10.1126/science.aab3574>, 2015.
- 1295 Tiner, R. W.: Global Distribution of Wetlands, in: *Encyclopedia of Inland Waters*, edited by: Likens, G. E., 3, Elsevier, 526-530, <https://doi.org/10.1016/B978-012370626-3.00068-5>, 2009.
- Tiner, R. W.: *Dichotomous Keys and Mapping Codes for Wetland Landscape Position, Landform, Water Flow Path, and Waterbody Type Descriptors: Version 3.0*, U.S. Fish and Wildlife Service, Northeast Region, Hadley, MA, 65 pp., 2014.
- Tiner, R. W.: Wetlands: An overview, in: *Remote Sensing of Wetlands: Applications and Advances*, edited by: Tiner, R. W.,  
1300 Lang, M., and Klemas, V. V., CRC Press, ISBN 9780429183294, 2015.
- Tiner, R. W.: *Wetland Indicators: A Guide to Wetland Formation, Identification, Delineation, Classification, and Mapping*, 2nd ed., CRC Press, Boca Raton, <https://doi.org/10.1201/9781315374710>, 2016.
- Tootchi, A., Jost, A., and Ducharme, A.: Multi-source global wetland maps combining surface water imagery and groundwater constraints, *Earth Syst. Sci. Data*, 11, 189-220, <https://doi.org/10.5194/essd-11-189-2019>, 2019.
- 1305 van Asselen, S., Verburg, P. H., Vermaat, J. E., and Janse, J. H.: Drivers of Wetland Conversion: a Global Meta-Analysis, *Plos One*, 8, <https://doi.org/10.1371/journal.pone.0081292>, 2013.
- Verhoeven, J. T. and Setter, T. L.: Agricultural use of wetlands: opportunities and limitations, *Ann. Bot-London*, 105, 155-163, <https://doi.org/10.1093/aob/mcpl172>, 2010.
- Verpoorter, C., Kutser, T., Seekell, D. A., and Tranvik, L. J.: A global inventory of lakes based on high-resolution satellite  
1310 imagery, *Geophys. Res. Lett.*, 41, 6396-6402, <https://doi.org/10.1002/2014gl060641>, 2014.
- Vörösmarty, C. J., McIntyre, P. B., Gessner, M. O., Dudgeon, D., Prusevich, A., Green, P., Glidden, S., Bunn, S. E., Sullivan, C. A., Liermann, C. R., and Davies, P. M.: Global threats to human water security and river biodiversity, *Nature*, 467, 555-561, <https://doi.org/10.1038/nature09440>, 2010.
- Wang, J. D., Walter, B. A., Yao, F. F., Song, C. Q., Ding, M., Maroof, A., Zhu, J. Y., Fan, C. Y., McAlister, J. M., Sikder,  
1315 S., Sheng, Y. W., Allen, G. H., Crétaux, J. F., and Wada, Y.: GeoDAR: georeferenced global dams and reservoirs dataset for bridging attributes and geolocations, *Earth Syst. Sci. Data*, 14, 1869-1899, <https://doi.org/10.5194/essd-14-1869-2022>, 2022.
- Woodwell, G. M., Rich, P. H., and Hall, C. A.: Carbon in estuaries, *Brookhaven Symp Biol*, 221-240, PMID: 4807338, 1973.
- 1320 Worthington, T. A., Spalding, M., Landis, E., Maxwell, T. L., Navarro, A., Smart, L. S., and Murray, N. J.: The distribution of global tidal marshes from Earth observation data, *Global. Ecol. Biogeogr.*, <https://doi.org/10.1111/geb.13852>, 2024.



- Xi, Y., Peng, S. S., Ciais, P., and Chen, Y. H.: Future impacts of climate change on inland Ramsar wetlands, *Nat. Clim. Change.*, 11, 45-51, <https://doi.org/10.1038/s41558-020-00942-2>, 2021.
- 1325 Xu, J. R., Morris, P. J., Liu, J. G., and Holden, J.: PEATMAP: Refining estimates of global peatland distribution based on a meta-analysis, *Catena*, 160, 134-140, <https://doi.org/10.1016/j.catena.2017.09.010>, 2018.
- Yamazaki, D., Kanae, S., Kim, H., and Oki, T.: A physically based description of floodplain inundation dynamics in a global river routing model, *Water Resour. Res.*, 47, 10.1029/2010wr009726, 2011.
- Yamazaki, D., Trigg, M. A., and Ikeshima, D.: Development of a global ~90 m water body map using multi-temporal Landsat images, *Remote Sens. Environ.*, 171, 337-351, <https://doi.org/10.1016/j.rse.2015.10.014>, 2015.
- 1330 Yu, Q. Y., You, L. Z., Wood-Sichra, U., Ru, Y. T., Joglekar, A. K. B., Fritz, S., Xiong, W., Lu, M., Wu, W. B., and Yang, P.: A cultivated planet in 2010-Part 2: The global gridded agricultural-production maps, *Earth Syst. Sci. Data*, 12, 3545-3572, <https://doi.org/10.5194/essd-12-3545-2020>, 2020.
- Zhang, X., Liu, L. Y., Zhao, T. T., Chen, X. D., Lin, S. R., Wang, J. Q., Mi, J., and Liu, W. D.: GWL\_FCS30: a global 30 m wetland map with a fine classification system using multi-sourced and time-series remote sensing imagery in 2020, 1335 *Earth Syst. Sci. Data*, 15, 265-293, <https://doi.org/10.5194/essd-15-265-2023>, 2023.
- Zhang, X., Liu, L. Y., Zhao, T. T., Wang, J. Q., Liu, W. D., and Chen, X. D.: Global annual wetland dataset at 30 m with a fine classification system from 2000 to 2022, *Scientific Data*, 11, 310, <https://doi.org/10.1038/s41597-024-03143-0>, 2024.
- 1340 Zhang, Z., Fluet-Chouinard, E., Jensen, K., McDonald, K., Hugelius, G., Gumbrecht, T., Carroll, M., Prigent, C., Bartsch, A., and Poulter, B.: Development of the global dataset of Wetland Area and Dynamics for Methane Modeling (WAD2M), *Earth Syst. Sci. Data*, 13, 2001-2023, <https://doi.org/10.5194/essd-13-2001-2021>, 2021.